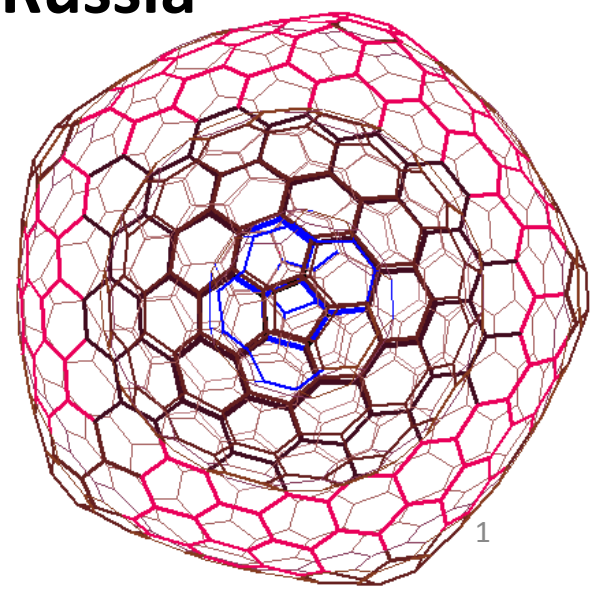
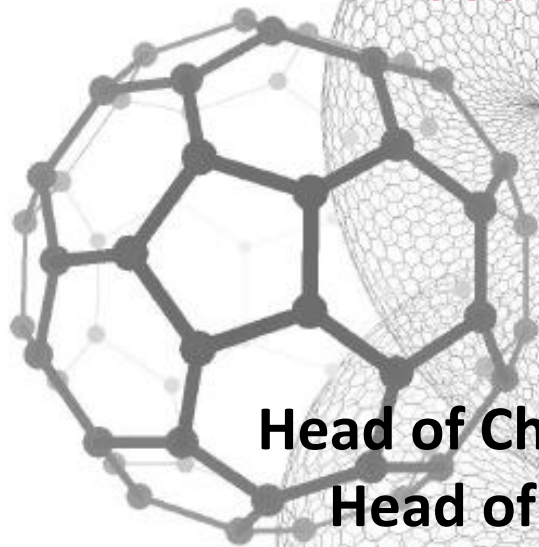
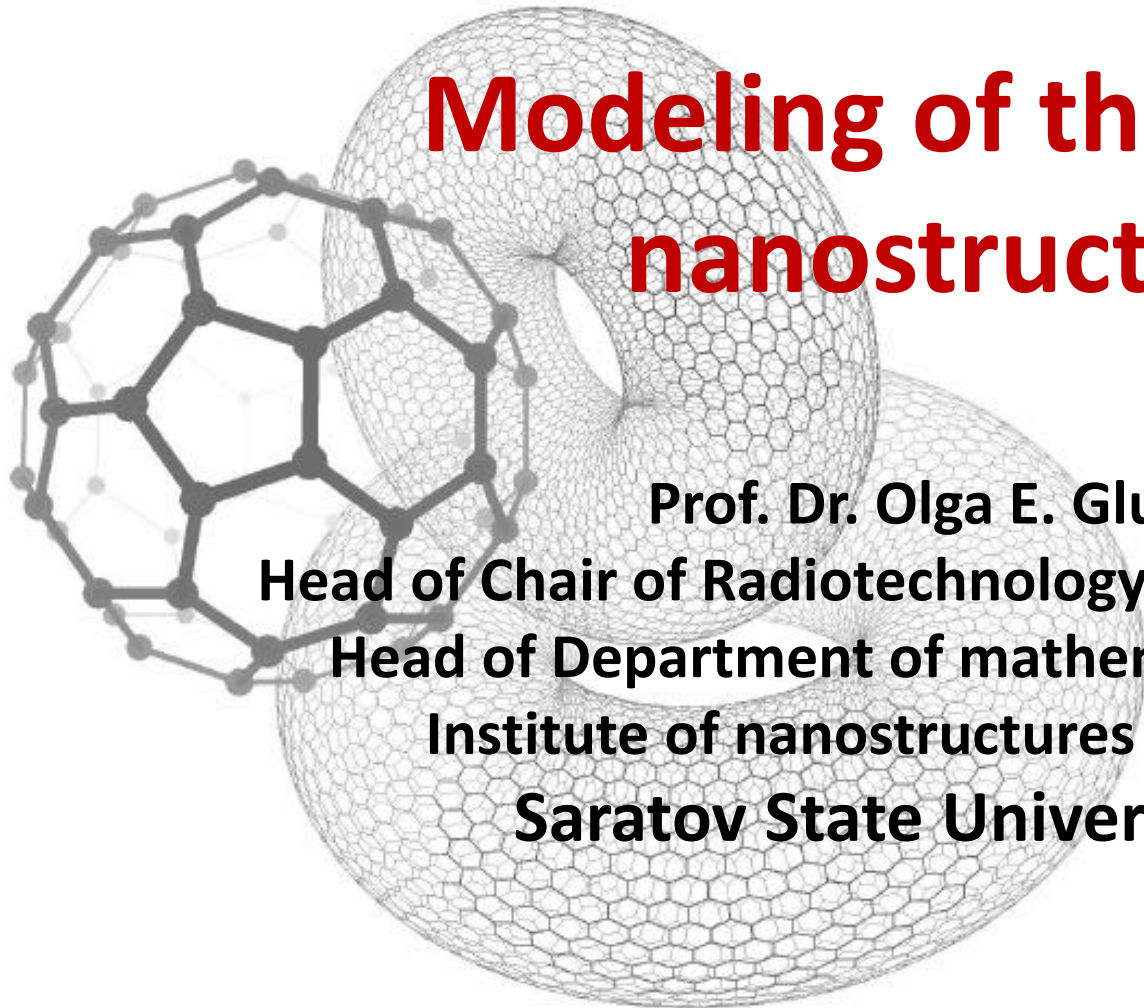


Modeling of the carbon nanostructures

**Prof. Dr. Olga E. Glukhova,
Head of Chair of Radiotechnology and Electrodynamics,
Head of Department of mathematical modeling of
Institute of nanostructures and biosystems
Saratov State University, Russia**

glukhovaoe@info.sgu.ru





Department of Computer Simulations

High-Performance Computing Division

Parallel Computing Algorithms
Supercomputers maintenance
Databases construction and maintenance

Mathematical Modeling Division

FEM Modeling :
Biomechanics;
Construction mechanics;
Solid structures mechanics;
Structural mechanics;
Composite mechanics

Mechanics of Nanostructures :
Mechanical properties of nanostructures;
Mechanical properties of bionanoobjects;
Multiscale modeling

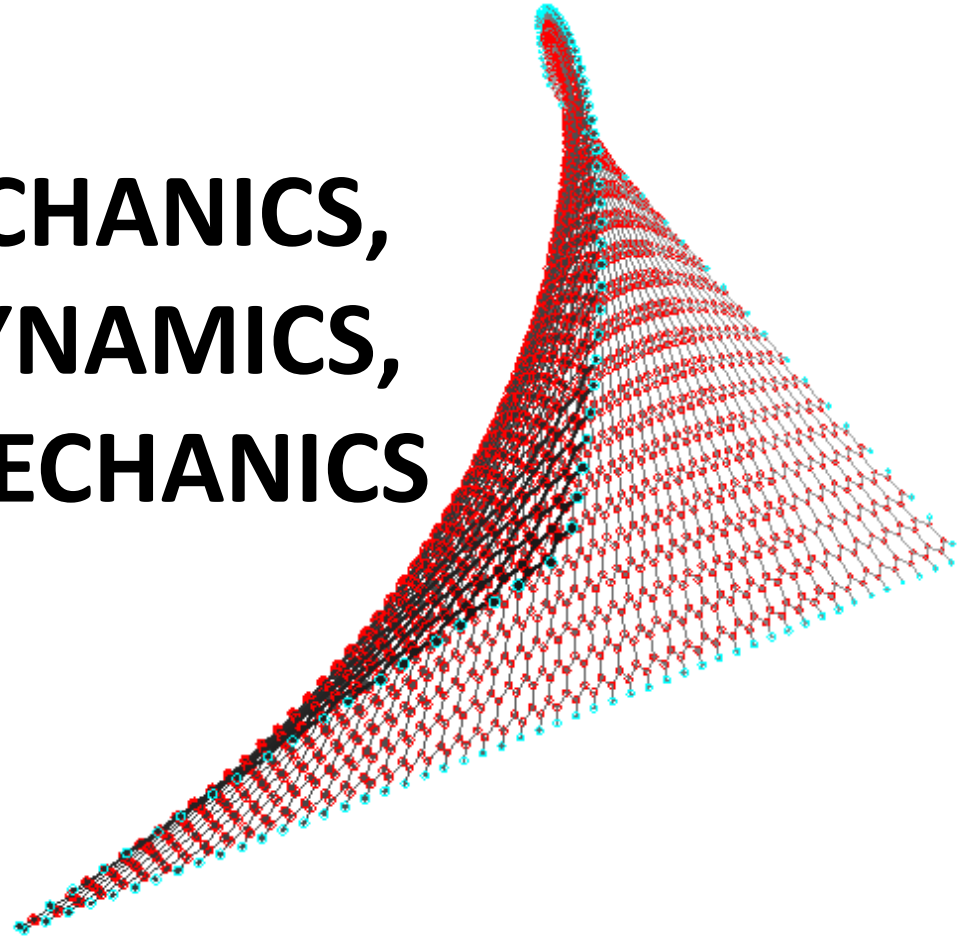
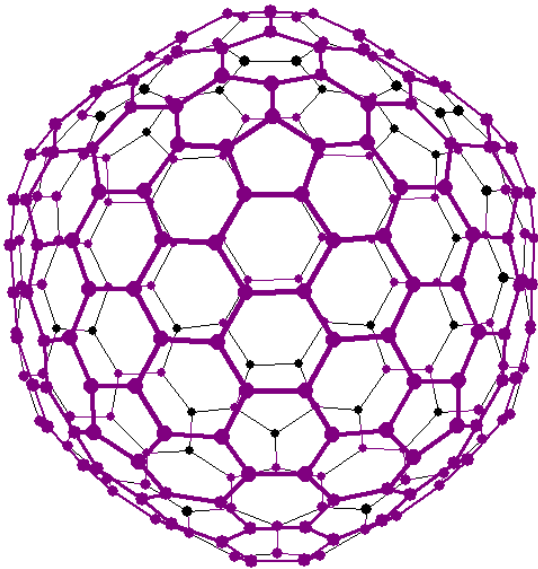
Nanoelectronics:
Electronic structure;
Emission properties;
Electronic conductivity

Radiotechnology and Electrodynamics Chair

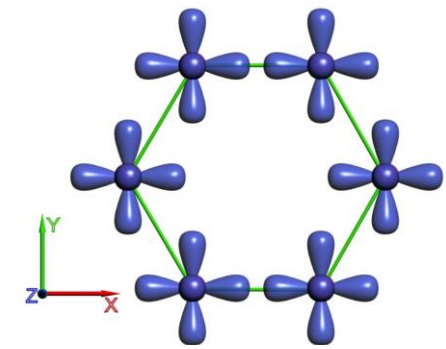
- Research fields:
- Modeling of nanodevices, based on carbon nanoclusters, nanoelectronics, nanobiosystems mechanics, molecular electronics, mathematical modeling of physical processes.
- Microtron (electron accelerator) physical processes;
- Theoretical and applied electrodynamics of micro- and extremely high wave frequencies;
- Radiotechnical research methods of superconductors as the objects for recording, storage and processing of information and optimization of transformer chains for powerful impulse generators;
- 3D displays, mathematical logic methods, mathematical modeling in biology and medicine.



COMPUTATIONAL METHODS: QUANTUM MECHANICS, MOLECULAR DYNAMICS, MOLECULAR MECHANICS



1) Tight-binding method



The TB method was earlier implemented to study a stability of carbon. The energy of a system of ion cores and valence electrons is written as

$$E_{tot} = E_{bond} + E_{rep}. \quad (1)$$

Here the term E_{bond} is the bond structure energy that is calculated as the sum of energies of the single-particle occupied states. Those single-particle energies are known by solving the Schrodinger equation

$$\mathbf{H} |\psi_n\rangle = \epsilon_n |\psi_n\rangle, \quad (2)$$

where \mathbf{H} is the one-electron Hamiltonian, ϵ_n is the energy of the n th single-particle state.

The wave functions $|\psi_n\rangle$ can be approximated by linear combination

$$|\psi_n\rangle = \sum_{l\alpha} C_{l\alpha}^n |\phi_{l\alpha}\rangle, \quad (3)$$

where $\{\phi_{l\alpha}\}$ is an orthogonal basis set, l is the quantum number index and α labels the ions. This approximation is known as the method LCAO – linear combination of atomic orbits.

For example, the one-electron wave function of the compound C_n is given by the combination of the wave functions $|s\rangle, |p_x\rangle, |p_y\rangle, |p_z\rangle$:

$$|\psi\rangle = \sum_{i=1}^n c_i |s_i\rangle + \sum_{i=n+1}^{2n} c_i |p_{xi}\rangle + \sum_{i=2n+1}^{3n} c_i |p_{yi}\rangle + \sum_{i=3n+1}^{4n} c_i |p_{zi}\rangle,$$

N is the number of atoms.

For the tight-binding Hamiltonian, we use the Slater–Koster parameterization scheme for the electronic hopping matrix elements.

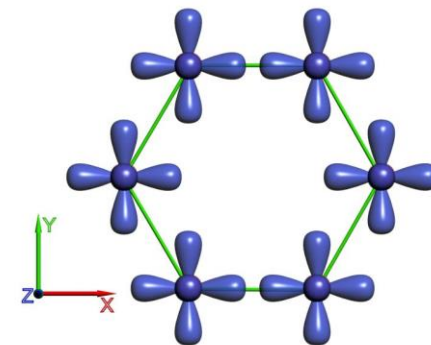
The equilibrium hopping integral is

$$V_{\alpha\beta}^0 = \langle \phi_{1\beta} | \mathbf{H} | \phi_{1\alpha} \rangle.$$

To describe the influence of environment on each atom we have included the scaling function. So, the matrix elements are calculated as (L. Goodwin, A. J. Skinner, and D. G. Pettifor, *Europhys.Lett.* 9 (1989) 701.)

$$V_{\alpha\beta}(r) = V_{\alpha\beta}^0 \left(\frac{p_3}{r} \right)^{p_1} \exp \left\{ p_1 \left[- \left(\frac{r}{p_2} \right)^{p_4} + \left(\frac{p_3}{p_2} \right)^{p_4} \right] \right\}, \quad (4)$$

where r is the distance between atoms.



The scaling function is known as the function of the two-center TB matrix element between two orbitals of symmetry l and l' placed on the atoms α and β . The parameter p_2 is equal the equilibrium interatomic distance. If the interatomic distance becomes equal the equilibrium distance the function is equal “1”.

Once that the single-particle energies are known by solving the secular problem (2).

$$E_{bond} = 2 \sum_{n=1}^{N_{occupied}} \varepsilon_n$$

Here “2” considers the electron spin.

The phenomenon energy

Term E_{rep} in Eq.(1) is the phenomenon energy that is a repulsive potential. It can be expressed as a sum of two-body potentials as

$$E_{\text{rep}} = \sum_{\alpha, \beta} V_{\text{rep}}(r_{\alpha\beta}), \quad (5)$$

where V_{rep} is pair potential between atoms at α and β . This two-body potential describes an interaction between bonded and nonbonded atoms.

The values of the parameters $V_{\alpha\beta}^0$, the atomic terms and p_n for carbon compounds are given in table.

Table 1

ε_s, eV	ε_p, eV	$V_{\text{ss}\sigma}^0, \text{eV}$	$V_{\text{sp}\sigma}^0, \text{eV}$	$V_{\text{pp}\sigma}^0, \text{eV}$	$V_{\text{pp}\pi}^0, \text{eV}$
-10,932	-5,991	-4,344	3,969	5,457	-1,938
p_1	$p_2, \text{\AA}$	$p_3, \text{\AA}$	p_4	p_5, eV	p_6
2,796	2,32	1,54	22	10,92	4,455

The repulsive pair potential is calculated by formula:

$$V_{\text{rep}}(r) = p_5 \left(\frac{p_3}{r} \right)^{p_6} \exp \left\{ p_6 \left[- \left(\frac{r}{p_2} \right)^{p_4} + \left(\frac{p_3}{p_2} \right)^{p_4} \right] \right\} \quad (6)$$

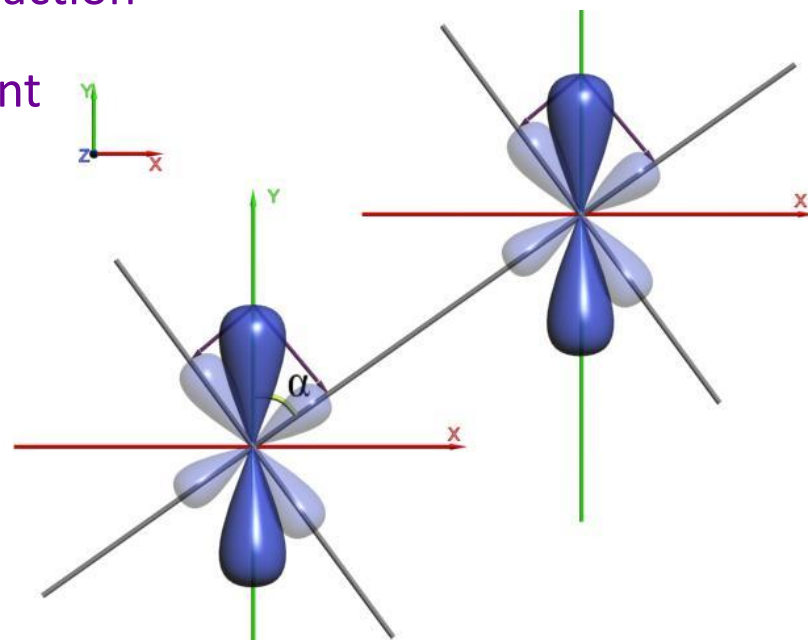
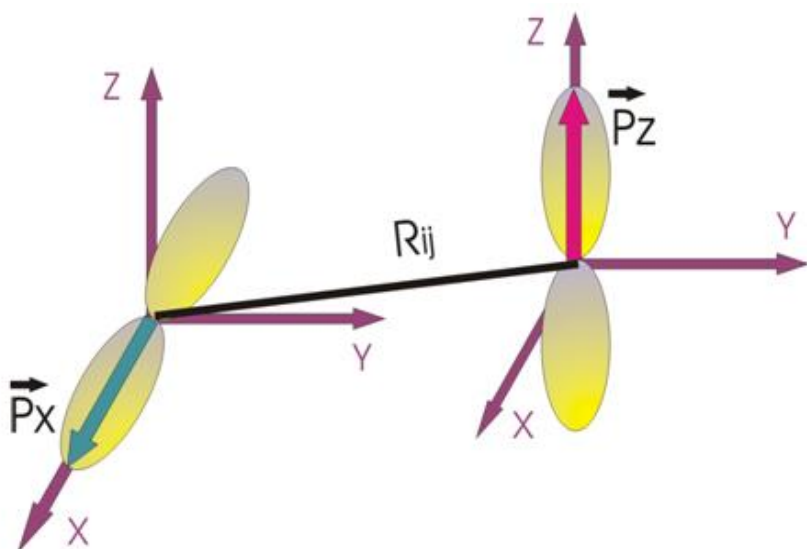
All parameters that define the phenomenon energy and were fitted from experimental data for fullerenes and carbon nanotubes.

Transferability to other carbon compounds was tested by comparison with ab initio calculations and experiments. Our parametrization provides the investigations of all modifications of carbon nanostructures. That provides also the study the molecular clusters, finite size structures with sp^2 , $sp^{2+\Delta}$, sp^3 .

O.E. Glukhova and A. I. Zhbanov . // Physics of Solid State (Springer). 2003. Vol. 45. P. 189-196
 O.E. Glukhova // Journal of Molecular Modeling. 2011. Volume 17. Issue 3. Page 573-576.

The transferable reproduction of the interaction between each atom and its environment

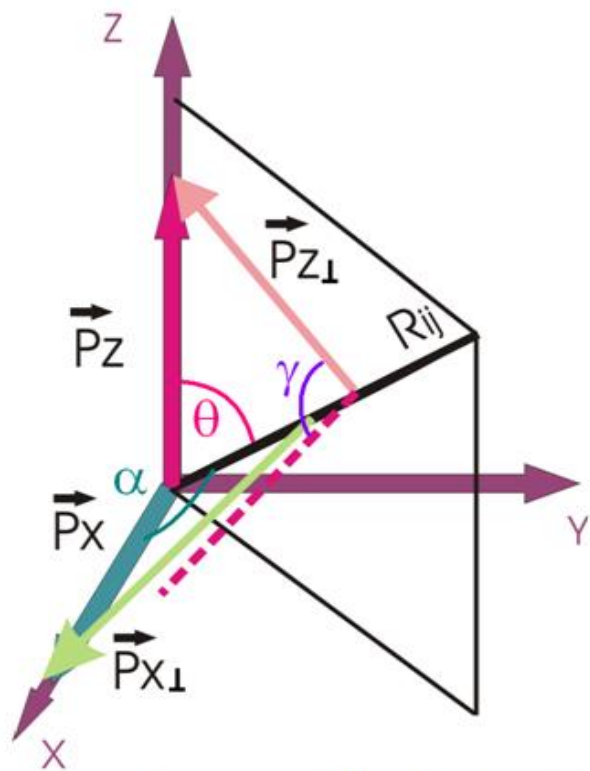
$$\begin{aligned} \vec{P}_x &= \vec{P}_{xD} + \vec{P}_{x\perp}, \quad \vec{P}_y = \vec{P}_{yD} + \vec{P}_{y\perp}, \\ \vec{P}_z &= \vec{P}_{zD} + \vec{P}_{z\perp}. \end{aligned} \quad (7)$$



Here \vec{P}_{xD} , \vec{P}_{yD} , \vec{P}_{zD} are projections to an iteratomic direction, $\vec{P}_{x\perp}$... are projections to an orthogonal direction.

So, to describe the interaction between P_z and P_x (see Fig.) we must write:

$$\vec{P}_x \cdot \vec{P}_z = \underbrace{\vec{P}_{xD} \cdot \vec{P}_{zD}}_{\sigma\text{-bonding}} + \underbrace{\vec{P}_{x\perp} \cdot \vec{P}_{z\perp}}_{\pi\text{-bonding}}. \quad (8)$$

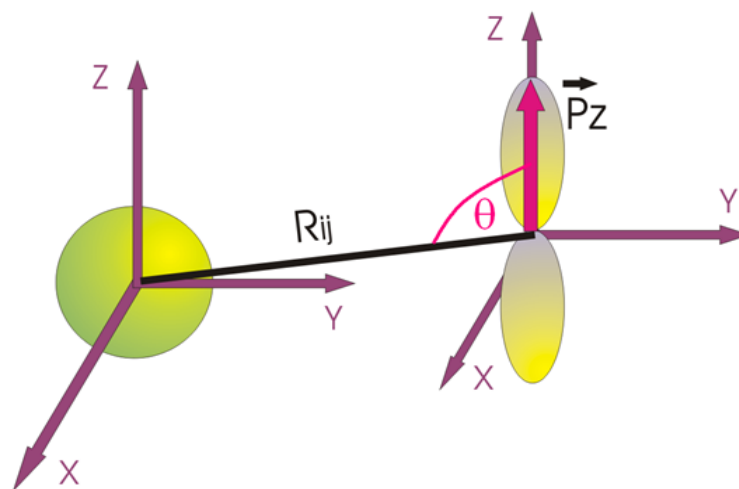


Projections of P_z - and P_x -vectors

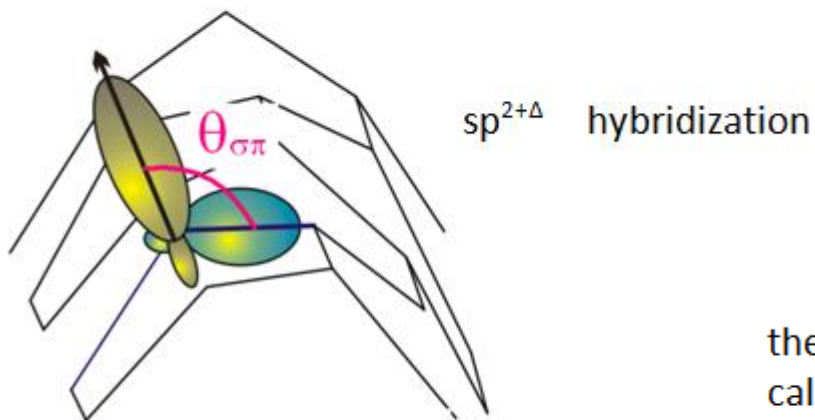
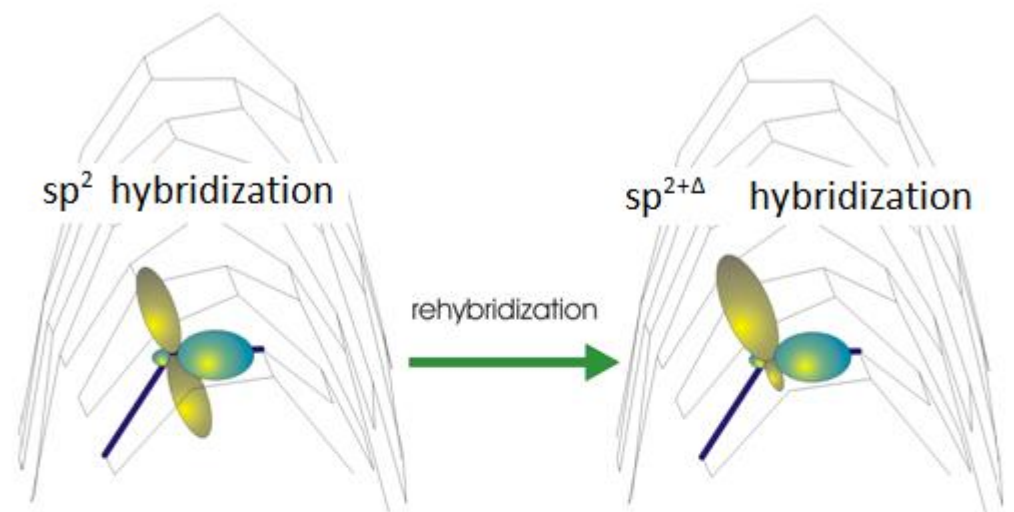
$$\cos \gamma = -\frac{\cos \alpha \cdot \cos \theta}{\sin \alpha \cdot \sin \theta}, \quad (9)$$

$$\begin{aligned} V_{P_x P_z}(r_{ij}) &= V_{P_x P_z}^{\sigma}(r_{ij}) \cdot \cos \alpha \cdot \cos \theta + V_{P_x P_z}^{\pi}(r_{ij}) \cdot \sin \alpha \cdot \sin \theta \cdot \cos \gamma = \\ &= V_{P_x P_z}^{\sigma}(r_{ij}) \cdot \cos \alpha \cdot \cos \theta + V_{P_x P_z}^{\pi}(r_{ij}) \cdot \sin \alpha \cdot \sin \theta \cdot \left(-\frac{\cos \alpha \cdot \cos \theta}{\sin \alpha \cdot \sin \theta} \right) = \\ &= \cos \alpha \cdot \cos \theta \left(V_{P_x P_z}^{\sigma}(r_{ij}) - V_{P_x P_z}^{\pi}(r_{ij}) \right) \end{aligned} \quad (10)$$

$$V_{S P_z}(r_{ij}) = V_{S P_z}^{\sigma}(r_{ij}) \cdot \cos \theta \quad (11)$$



Schematic representation of the interaction of P_z - and S - orbitals.



Degree of rehybridization is defined on the pyramidalization angle. This angle is calculated on formula:

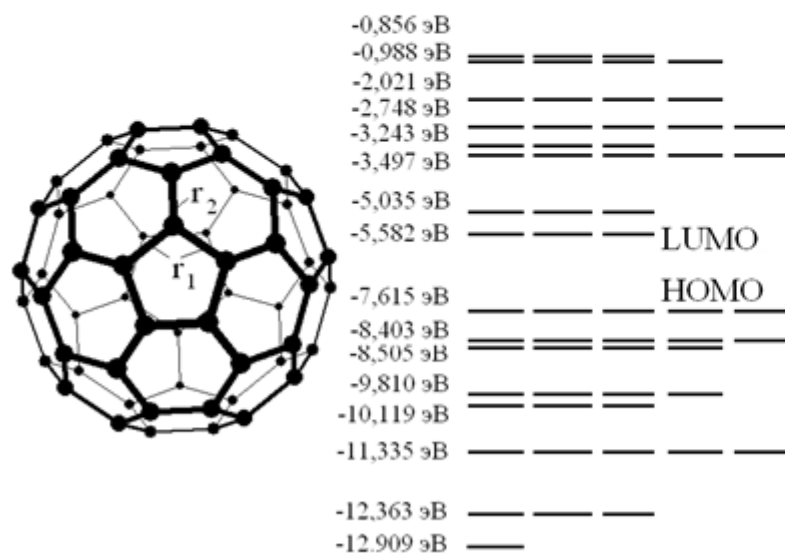
$$\theta_p = \theta_{\sigma\pi} - \frac{\pi}{2}.$$

The electron spectrum

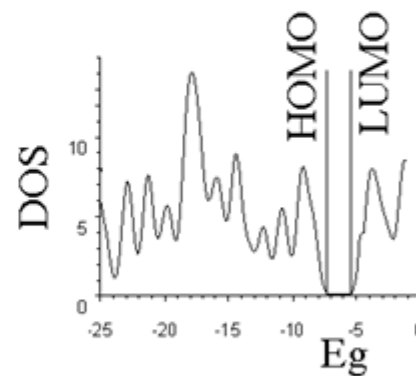
So, the presented transferable tight-binding potential and the described scheme to reproduce the electronic configuration and the local bonding geometry around each atom are well suited for computer simulations of covalently bonded systems in both gas-phase and condensed-phase systems.

We have tested our scheme by comparison with experiments for fullerene and some carbon nanotubes. In the table the spectra of the π -orbitals and density of states are presented.

Results are in reasonable agreement with experimental data.



Fullerene C_{60} and the spectra of π -orbitals



IP = 7.61 eV, E_g = 2 eV

r_1 = 1.45 Å, r_2 = 1.40 Å.

Mechanical Modeling:

- 1) reactive empirical bond-order (REBO) method developed by Brenner

The entire system energy is described by the sum of the binding energy E_b , the torsional energy E_{tors} and the van der Waals energy E_{vdW} :

$$E_{tot} = E_b + E_{tors} + E_{vdW}.$$

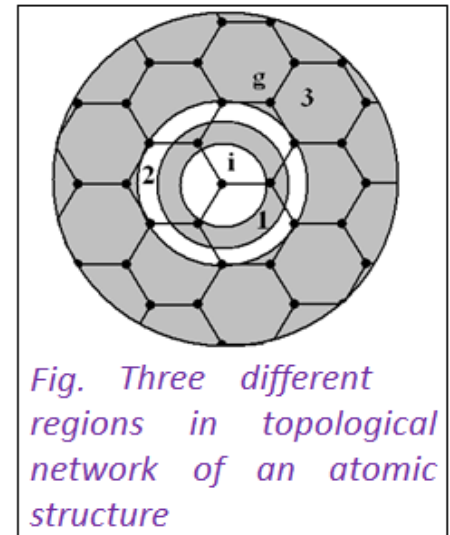


Fig. Three different regions in topological network of an atomic structure

Each pair of covalently bonded atoms interacts via a potential-energy:

$$E_b = \frac{1}{2} \sum_{i=1}^{Nat} \left(\sum_{j(\neq i)} (V_R(r_{ij}) - B_{ij} V_A(r_{ij})) \right).$$

This is the binding energy. Here V_R is the repulsive pair term, V_A is the attractive pair term, r_{ij} is the distance between the atom with number i and atom j from near region. The function B_{ij} is the many-body term. This term was introduced to describe the specificity of the σ - π interaction. So, the value of the binding energy depends on the position and chemical identity of atoms.

The torsional potential is given by the formula

$$E_{tors} = \frac{1}{2} \sum_{i=1}^{Nat} \left(\sum_{j \neq i} \left(\sum_{k \neq i, j} \left(\sum_{l \neq i, j, k} V_{tors}(\omega_{ijkl}) \right) \right) \right).$$

The torsional potential $V_{tors}(\omega_{ijkl})$ is given as a function of a dihedral angle ω . The torsion angle ω_{ijkl} is defined in the usual way as the angle between the plane defined by the vectors r_{ik} and r_{ij} and that defined by r_{ij} and r_{jl} . Here atoms j and k are given from intermediate (second) region and the atom l is given from far region.

Van der Waals energy E_{vdW} defines the interaction between non-bonded atoms:

$$E_{\text{vdW}} = \frac{1}{2} \sum_{i=1}^{\text{Nat}} \left(\sum_{j(\neq i)} V_{\text{vdW}}(r_{ij}) \right).$$

Van der Waals interaction energy may be described by the Lennard-Jones, Morse, Buckingham potentials and so on. We have implemented and compared Lennard-Jones and Morse potentials as the functions to define the van der Waals energy. We use Morse potential that is given by

$$V_{\text{Morse}}(r_{ij}) = D_e \left(\left(1 - \exp(-\beta(r_{ij} - r_e)) \right)^2 - 1 \right) + E_r \cdot \exp(-\beta' r_{ij}),$$

where D_e is the average bond energy, E_r is the repulsion nucleus energy, β, β' - parameters.

2) original empirical method

The total energy of carbon tubular nanostructure is defined by an empirical molecular-mechanical model as a polynomial whose components have their weight coefficient. The weight coefficients were chosen as the result of processing the experimental data on the elasticity and stiffness of defect-free nanotubes of simple forms. The valence force-field model, taking into account the van der Waals interaction of the unbound atoms, was taken at the basis:

$$E_{tot} = \sum k_r (r - r_0)^2 + \sum k_\theta (\theta - \theta_0)^2 + \sum \left(\frac{k_a}{r^{12}} - \frac{k_b}{r^6} \right)$$

Here, the first term takes into account the change of the binding length in the nanostructure in relation to the binding length in the graphite ($r_0 = 1,42\text{\AA}$). The second term considers the change of angles between the bindings in relation to the angle between the bindings in the graphite ($\theta = 120^\circ$), and the third term takes into account the van der Waals interaction (Lennard–Jones potential), K_r , K_θ , K_a , K_b – weight coefficients.

The weight coefficients of the carbon compounds as the solution of the minimax problem with the limitations were found in the following manner:

$$\min \max S(A), \quad \text{where } S(A) = \sum_{i=1}^3 |r_i - r_i^0|$$

Here $\{r_i\}$ is a set of C-C binding length, $\{r_i^0\}$ is a set of known (calculated and experimental) values, $A=(K_r, K_\theta, K_\omega, K_b)$ is a vector of varied parameters. The surface of the goal function was created to find the global minimum for every set $(K_r, K_\theta, K_\omega, K_b)$. The basis point was shifted corresponding to its surface contour.

Set $\{r_i\}$ was found with the help of nanostructure total energy by the coordinates of all atoms.

The values of weight coefficients were obtained in the result of the solution of the minimax problem (2) as follows:

$$K_r = 3.25 \cdot 10^2 \frac{\text{Joule}}{\text{m}^2}, \quad K_\theta = 4.4 \cdot 10^{-19} \frac{\text{Joule}}{\text{rad}^2}, \quad K_a = 4.0 \cdot 10^{-139} \frac{\text{Joule}}{\text{m}^{12}},$$

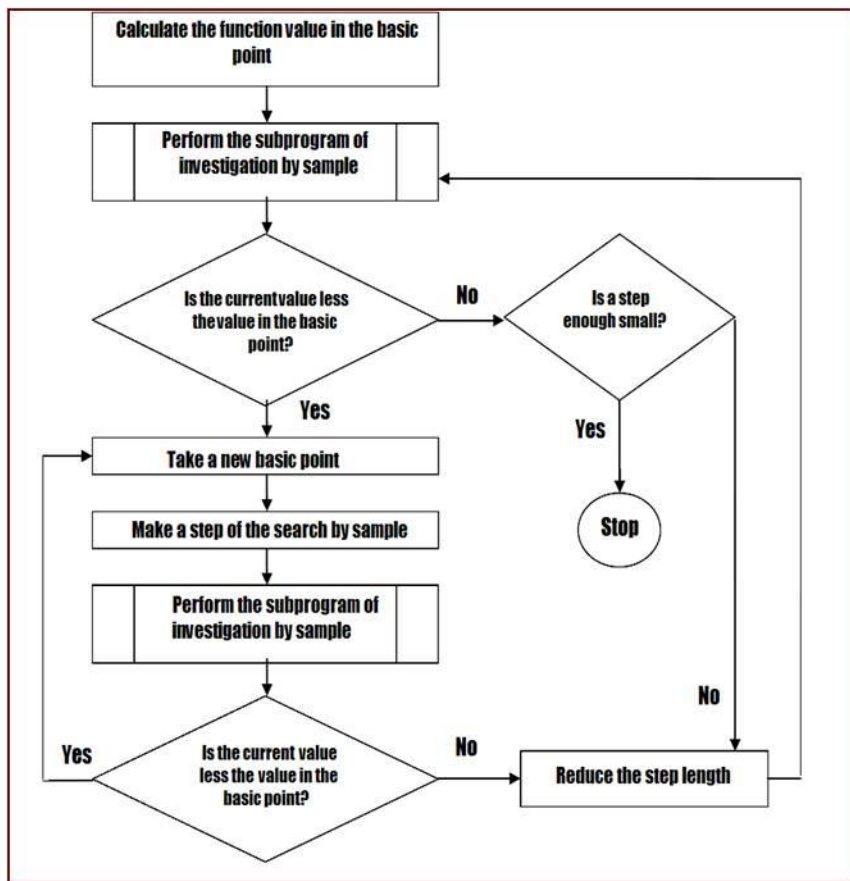
$$K_b = 1.5 \cdot 10^{-80} \frac{\text{Joule}}{\text{m}^6}.$$

To research the nanoribbons using tight-binding potential our own program was used. Our own program provides the calculation of the total energy of nanostructures, which consist of 500-5000 atoms. We have adapted our TB method to be able to run the algorithm on a parallel computing machine (computer cluster).

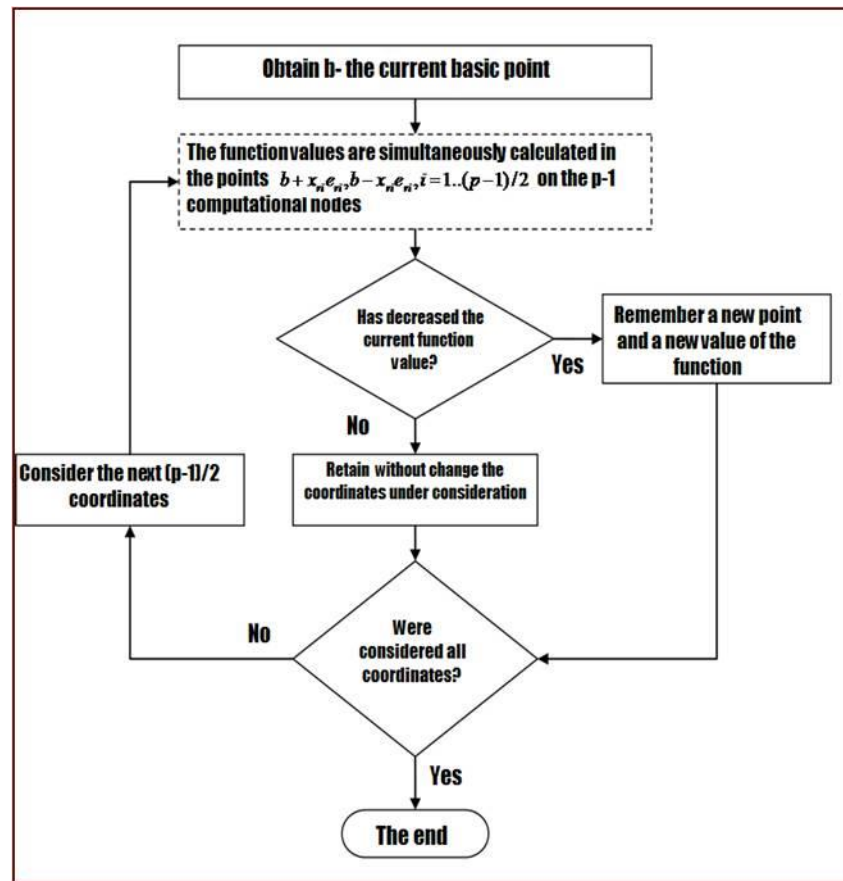
It's necessary to consider the available computing power.

We have a number of dual-processor servers which are the distributed SMP-system. MPI (stands for Message Passing Interface) was chosen as mechanism for implementing parallelism.

block diagram of the modified Hooke-Jeeves method



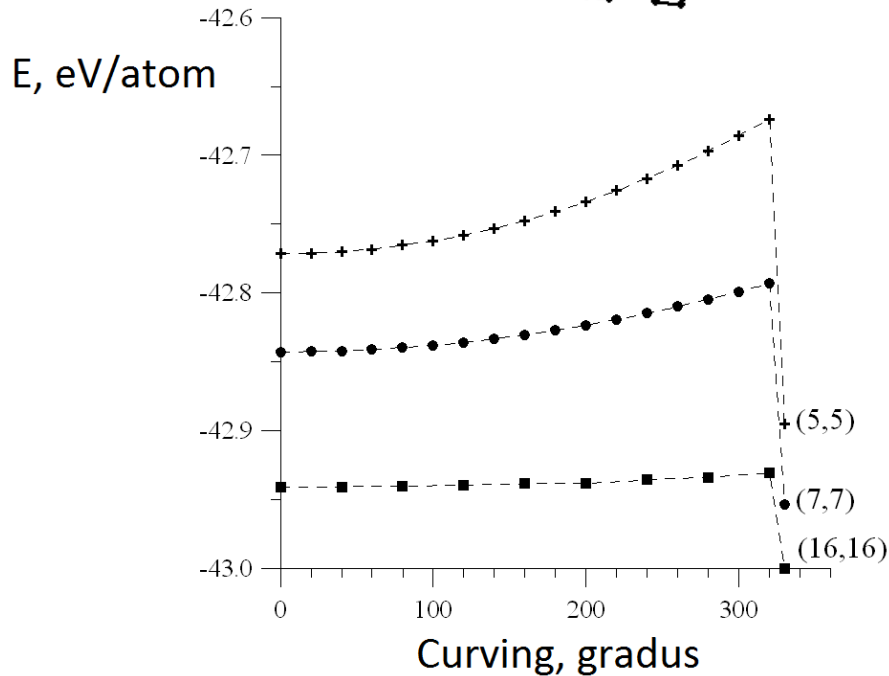
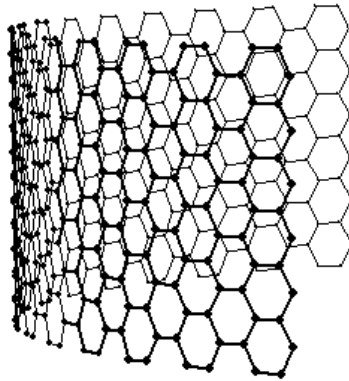
block diagram of the subprogram of investigation by sample



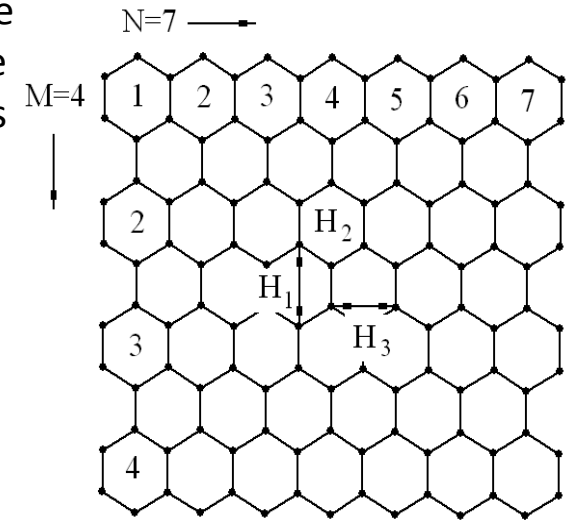
II. Graphene and CNT: electron and mechanical properties

Graphene: electron properties

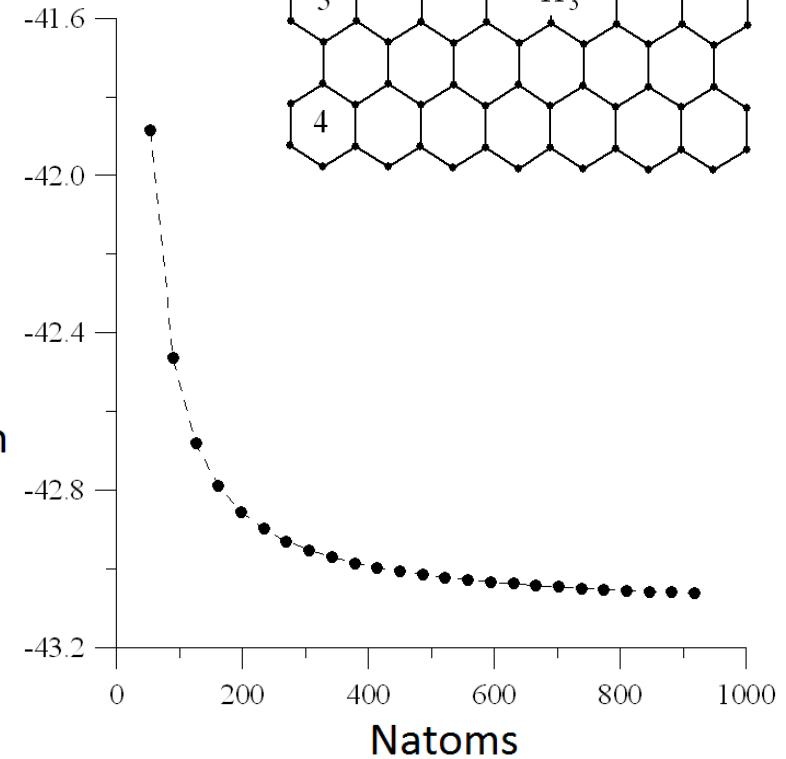
Scroll
of nanoribbon
(finite size effect)



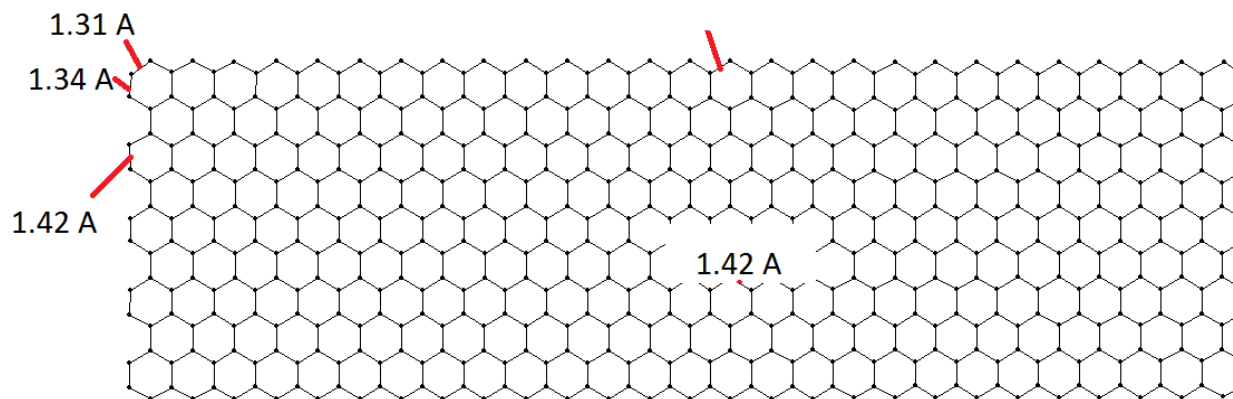
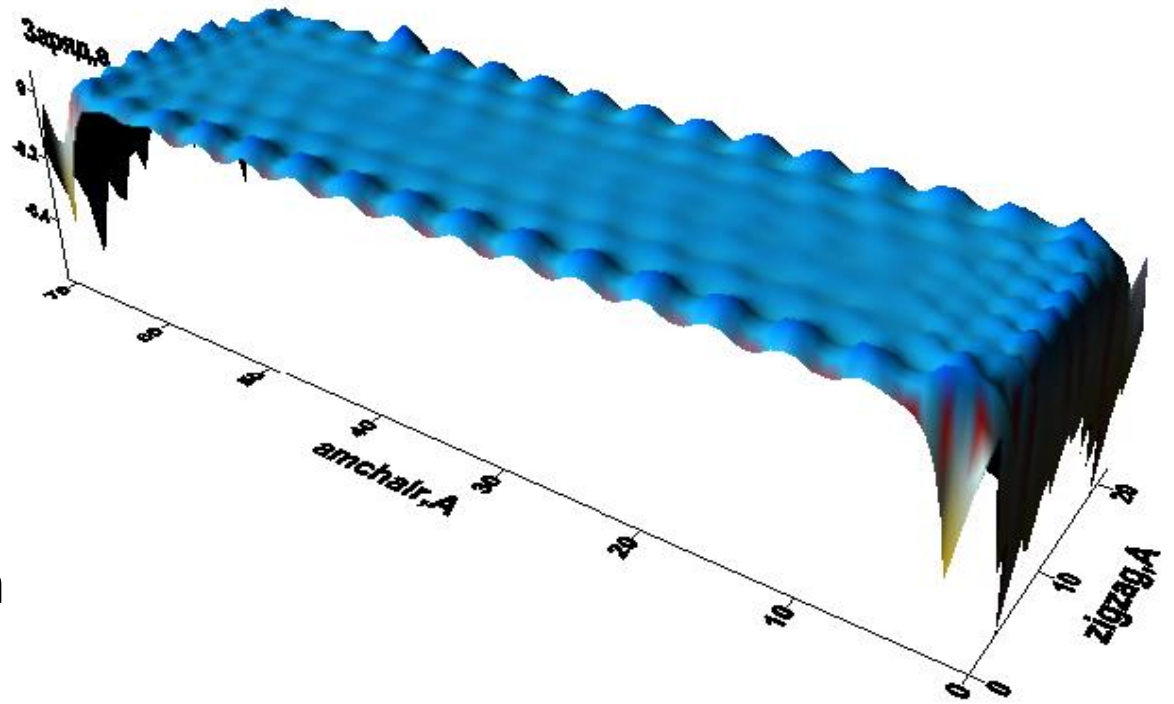
With increasing of the
number of atoms the
nanoribbon becomes
stable
(finite size effect)



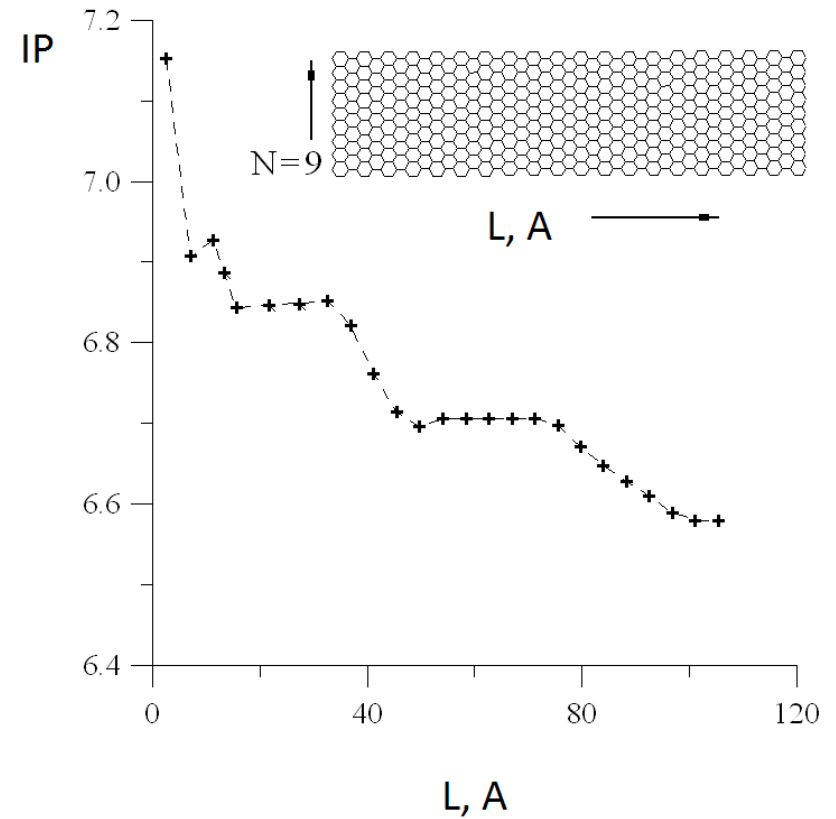
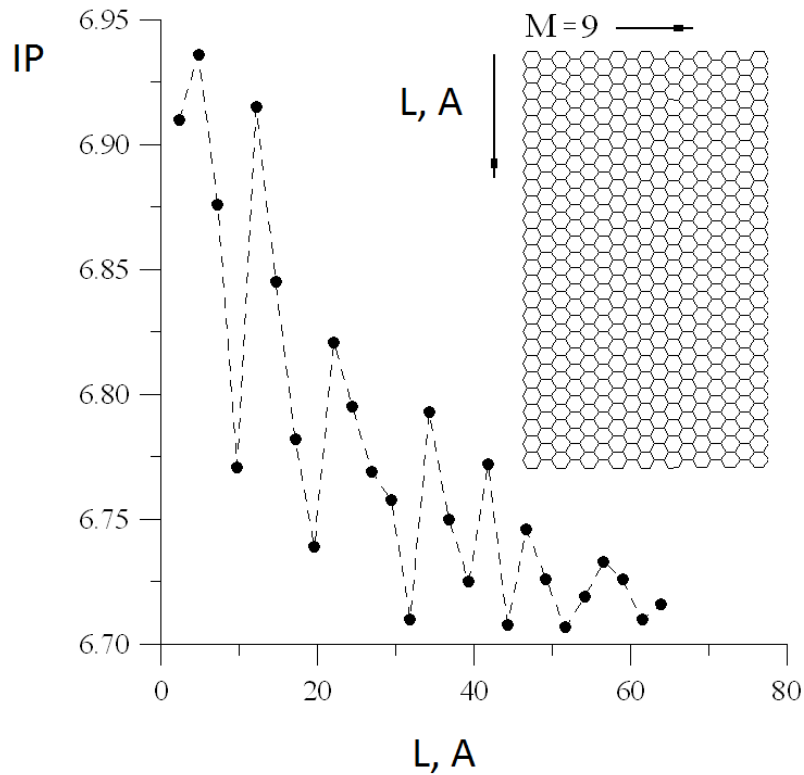
E_{atom} ,
eV/atom



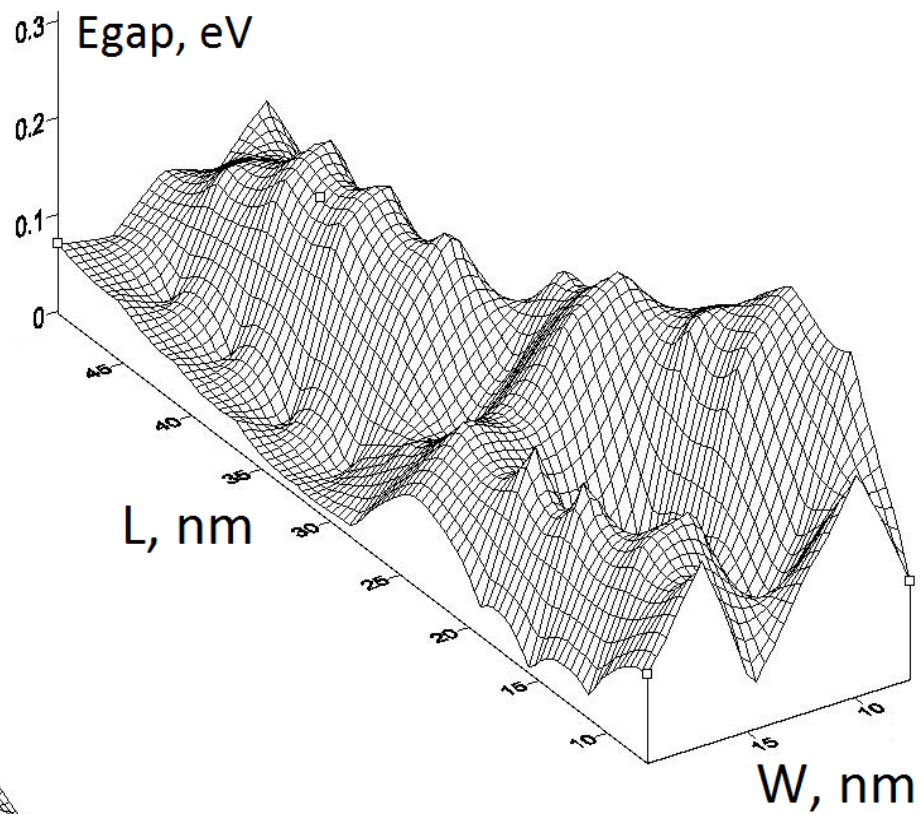
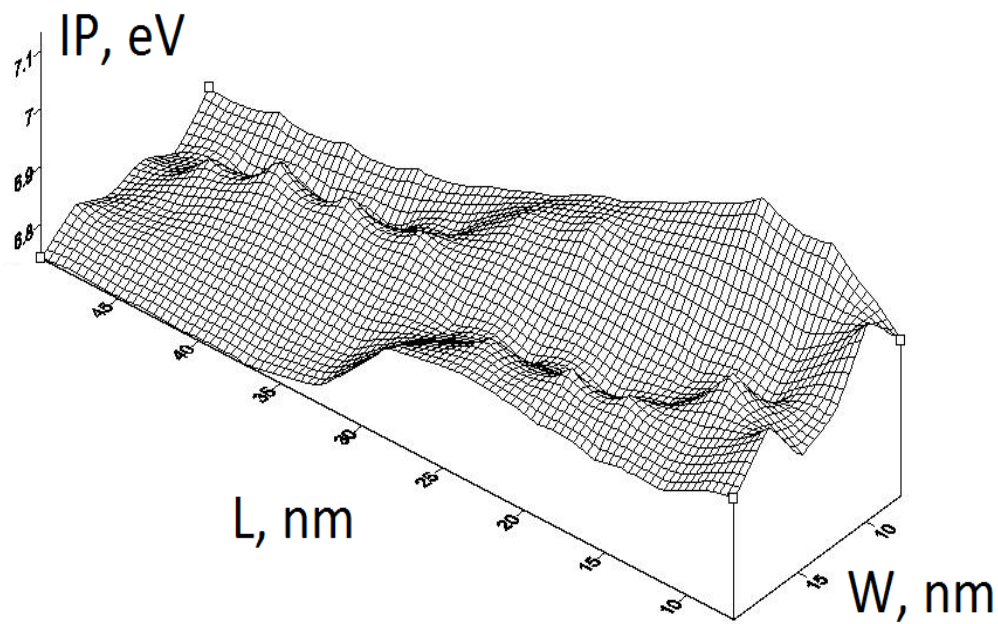
Density of Mulliken charge of carbon atoms of nanoribbon



The dependency of IP on the nanoribbon length (finite size effect)

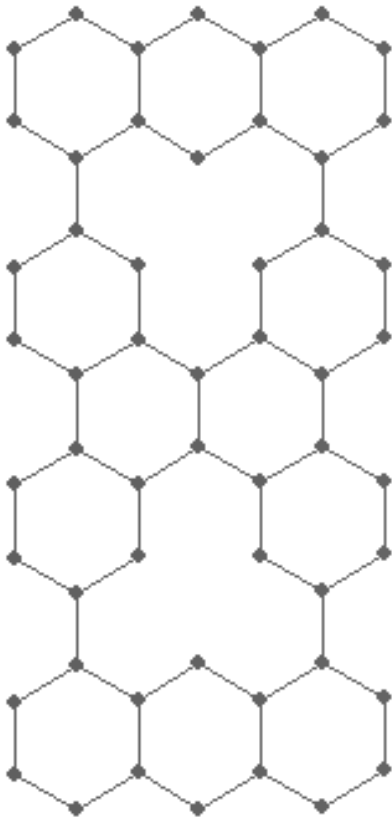


IP of nanoribbons



Energy gap of nanoribbons

Defected nanoribbons



The dependency of IP on the concentration of defect

	0 %	1,8 %	3,6 %	5,4 %
IP, eV	7,15	7,11	7,14	7,15

The dependency of the energy gap on the concentration of defect

	0 %	1,8 %	3,6 %	5,4 %
E _{gap} , eV	0,28	0,14	0,07	0,03

Nanotubes: electron properties

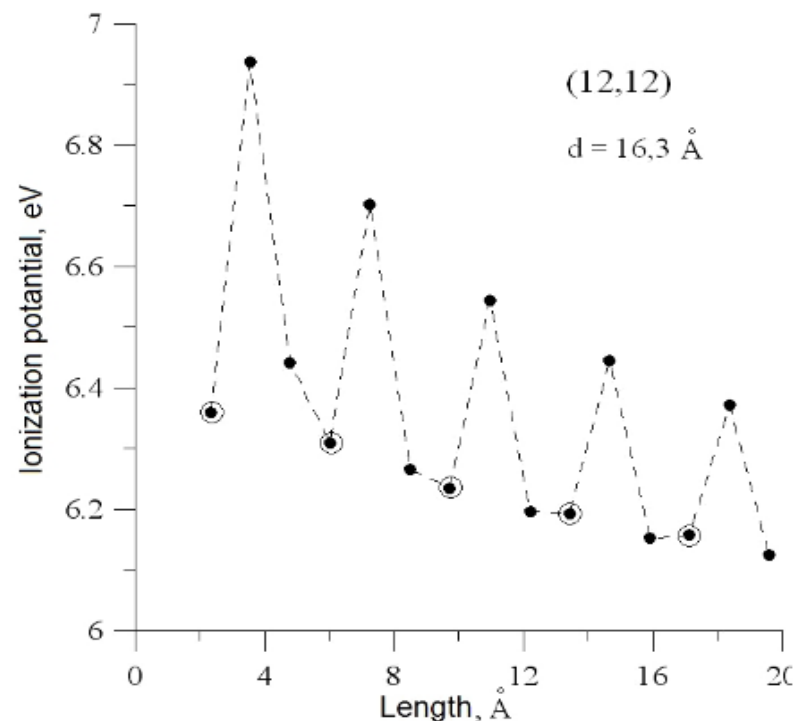
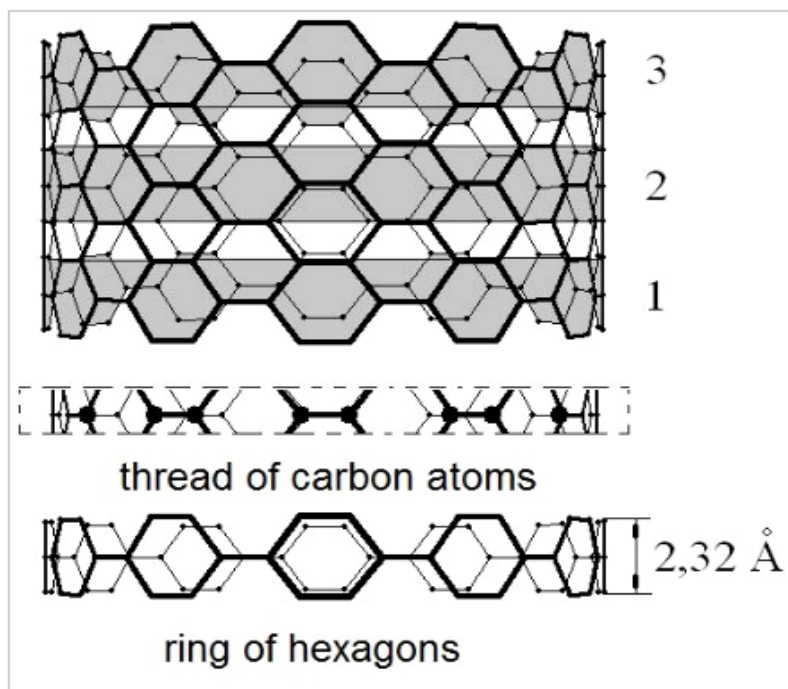
Nova Publisher (New York): «Carbon Nanotubes: Synthesis and Properties» (Editors: Ajay Kumar Mishra)

Chapter 15. Classification of Thin Achiral Carbon Nanotubes and Regularity their Electronic Structure

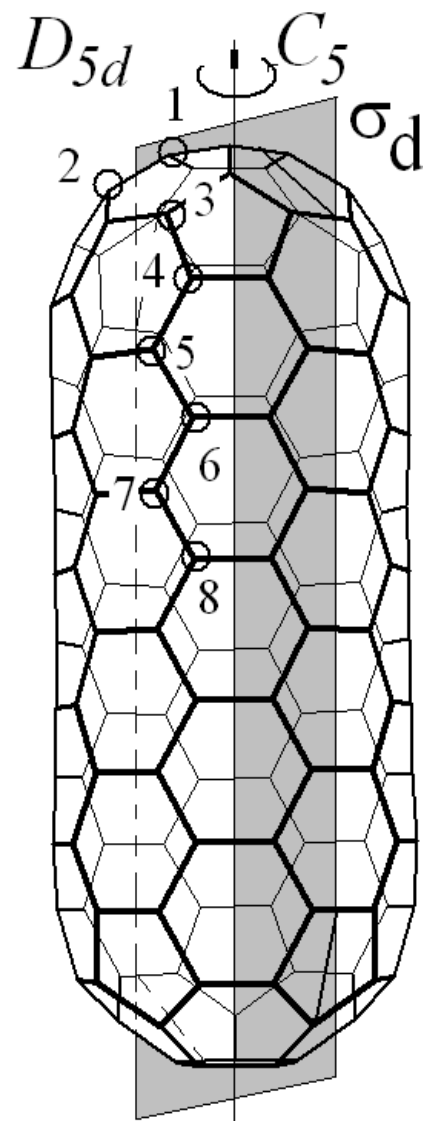
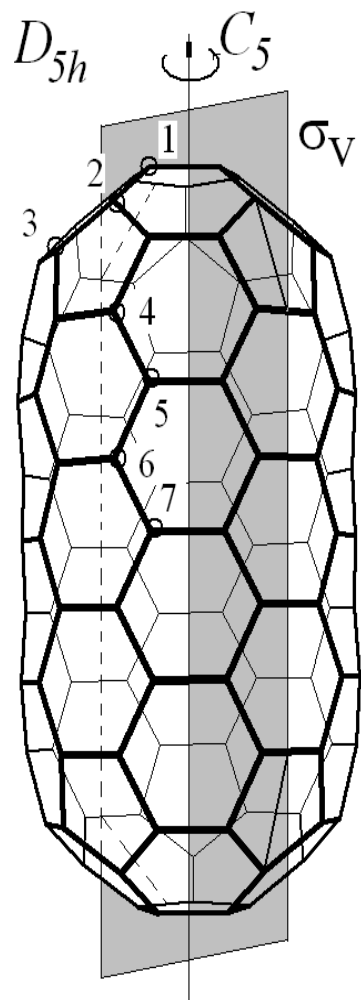
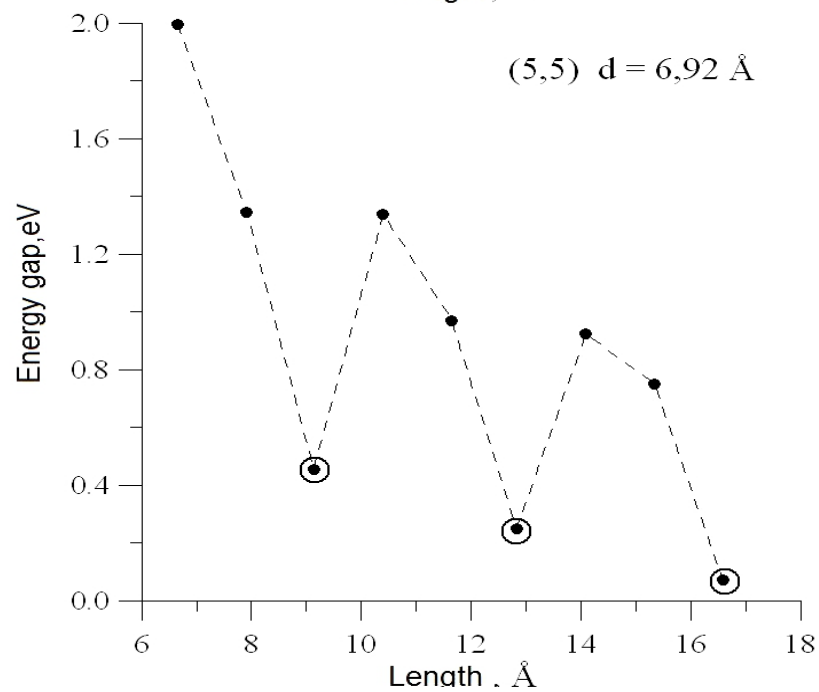
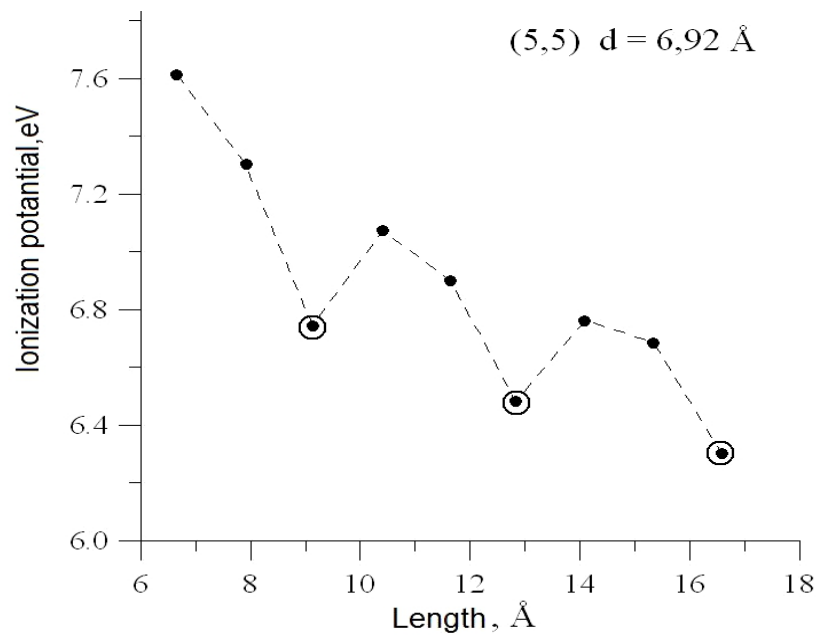
(Olga E. Glukhova, Department of Physics, Saratov State University, Saratov, Russia)

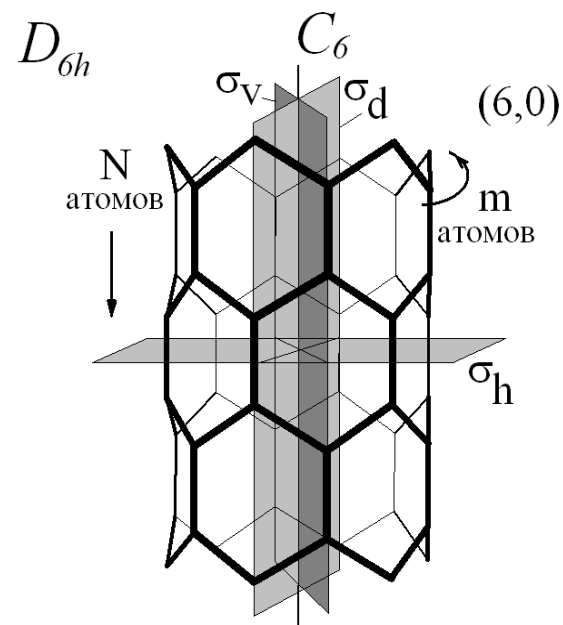
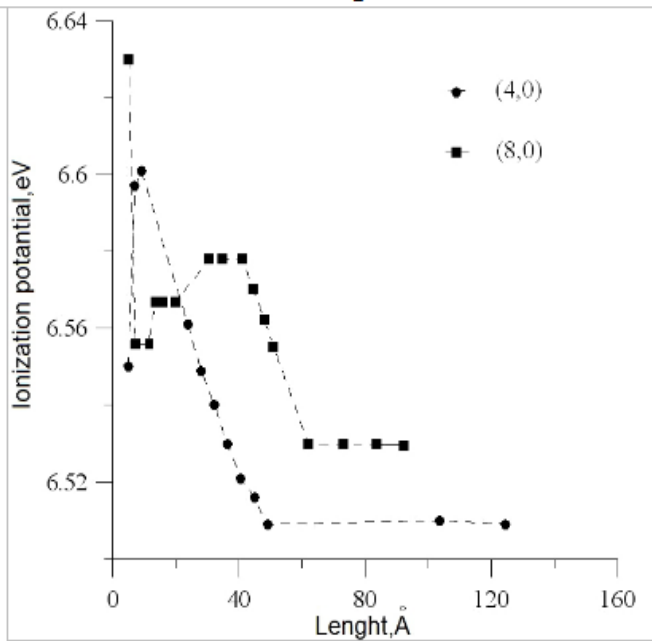
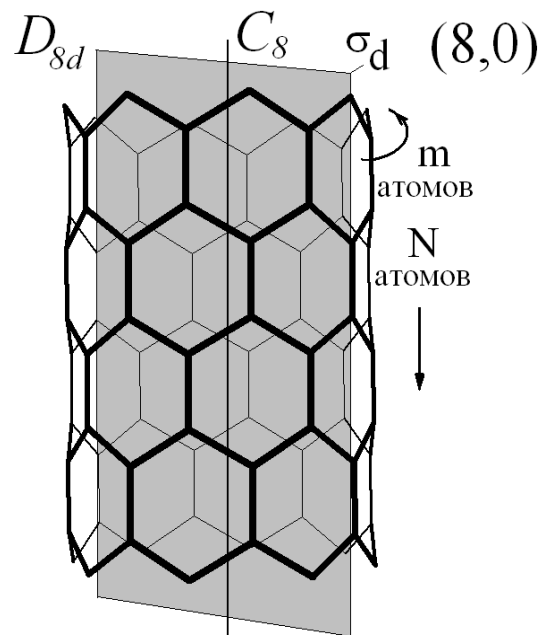
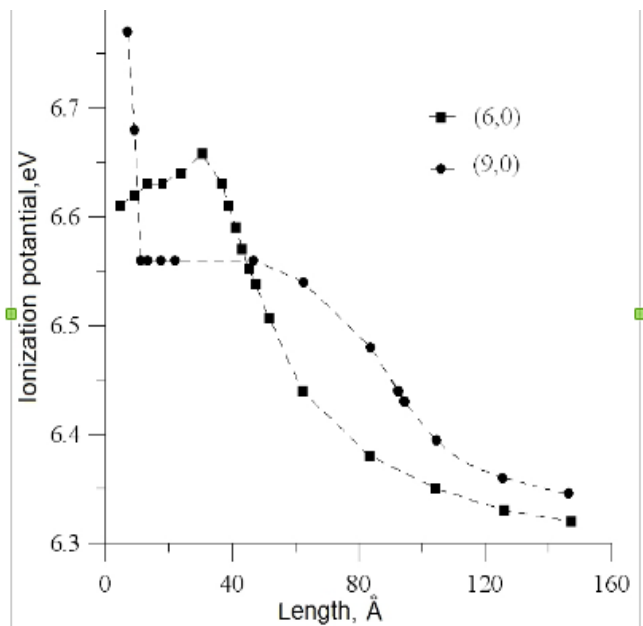
Series: Nanotechnology Science and Technology

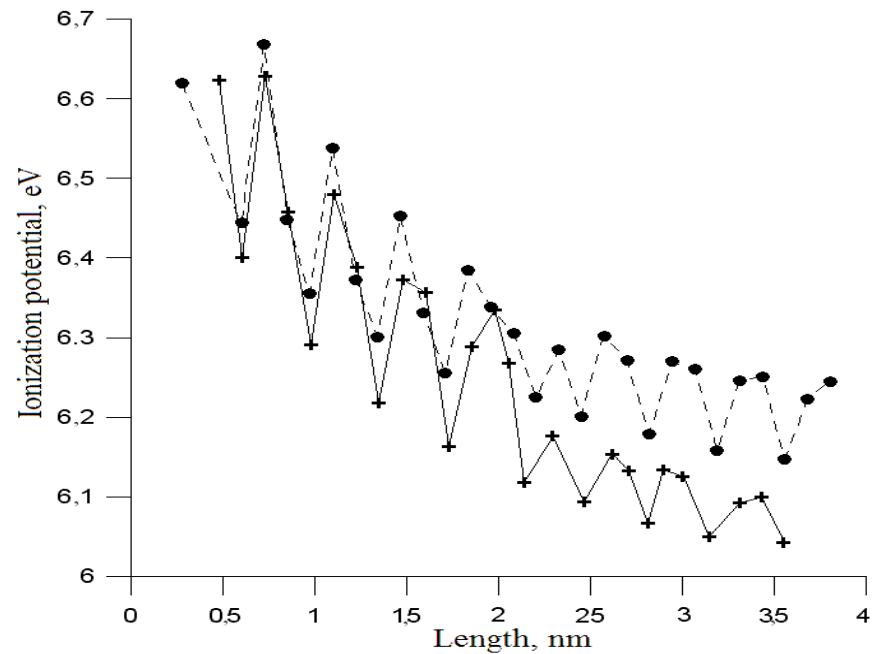
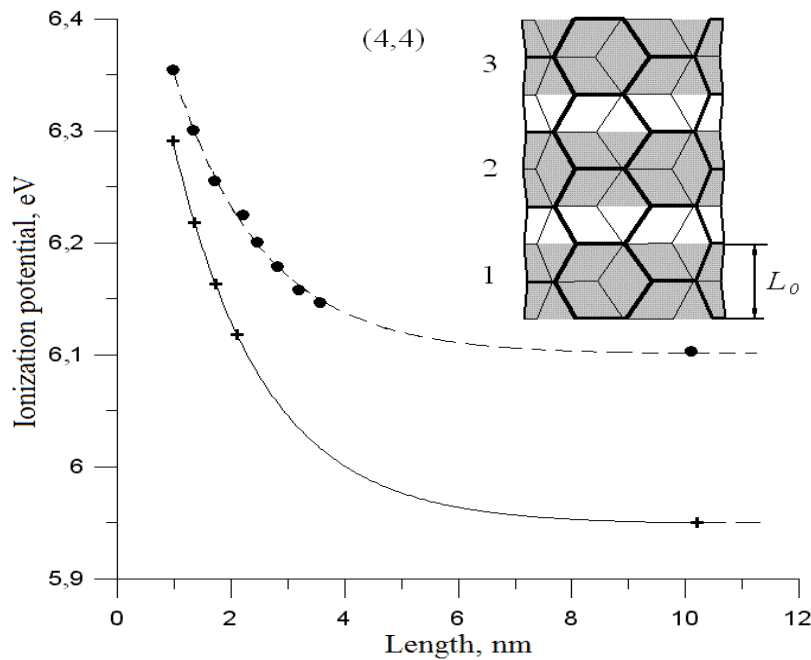
Binding: Hardcover **Pub. Date:** 2012 4th Quarter **Pages:** 7 x 10 (NBC - C) **ISBN:** 978-1-62081-914-2 **Status:** AN



The change of the ionization potential of the *armchair* nanoclusters with the length (for the fixed diameter): a) the cluster (3,3), b) the cluster (12,12). The length increases by means of attachment of the fibers of carbon atoms (dotted line) or by the rings of hexagons (the points marked by the circles).

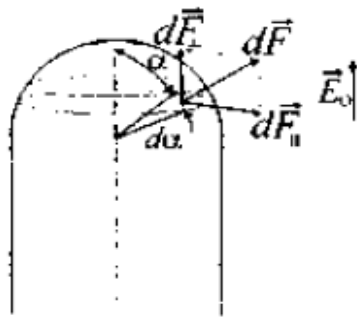




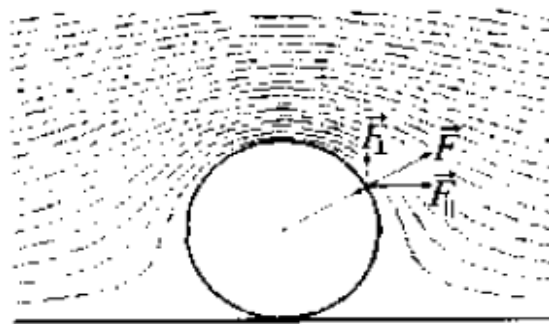


Dependence of the ionization potential of CNT (4,4) on the skeleton length:

(● – in absence of field, + – in electric field of ~ 3 V/nm)



(a)



(b)

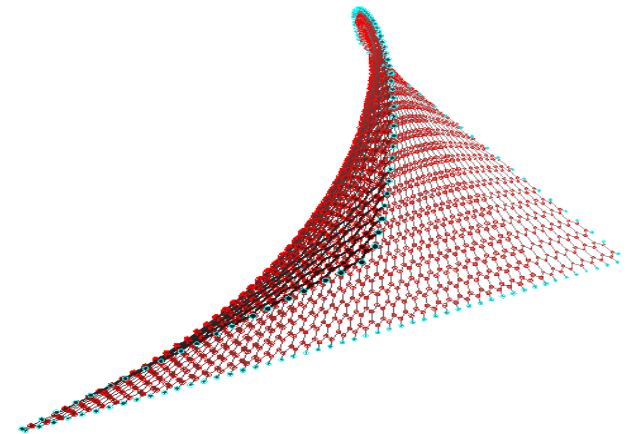
$$F = \epsilon_0 \frac{E_{\max}^2 \pi d^2}{8} \int_0^{\pi/2} (1 - A\alpha^2)^2 \sin 2\alpha \, d\alpha.$$

For example, assuming $R > 500 \text{ \AA}$, $d \approx 10 \text{ \AA}$, $H = 1000 \text{ \AA}$, $L = 200 \text{ \mu m}$, anode voltage $U_a = 8000 \text{ \AA}$, leads to $\beta = 115$, $E_0 = 4 \times 10^7 \text{ V/m}$, $E_{\max} = 4.6 \times 10^9 \text{ V/m}$. Hence, $F = 0.054 \text{ nN}$.

Ponderomotive forces acting on (a) vertically and (b) horizontally oriented nanotube.

III. MECHANICAL PROPERTIES

Study of deformations and elastic properties of nanoparticles and nanoribbons was implemented on the following algorithm



- 1) Optimization of atomic structure by entire system energy minimization on atomic coordinates (the atomic structure obtained from previous optimization);
- 2) Tension or compression of the atomic network of nanoribbon and reoptimization of atomic structure with fixed atoms on the nanoribbon ends;
- 3) Calculation the Young's pseudo-modulus for the elastic tension of nanoribbon on 1% on formula:

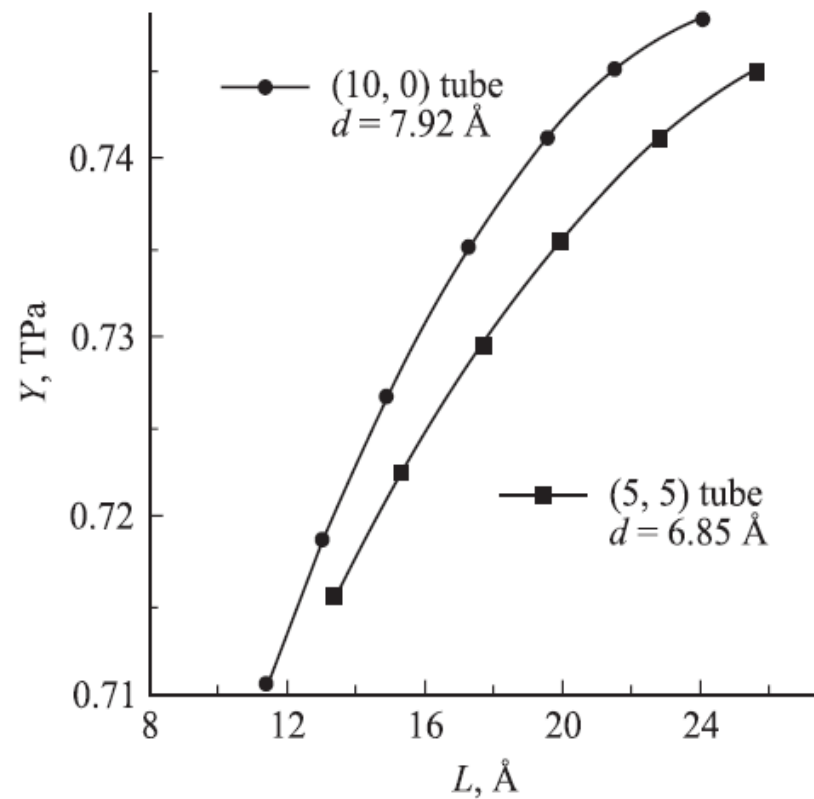
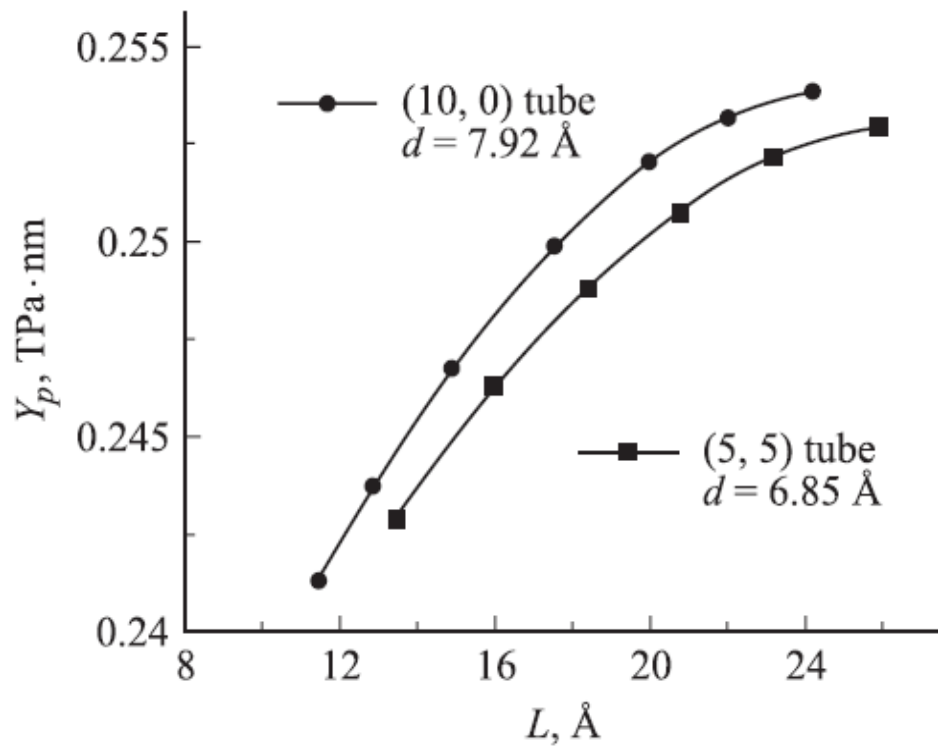
$$Y_p = \frac{F}{D} \frac{L}{\Delta L}$$

where a deformation force is given by $F = \frac{2\Delta E}{\Delta L}$. Here ΔE is the strain energy, namely, the total energy at a given axial strain minus the total.

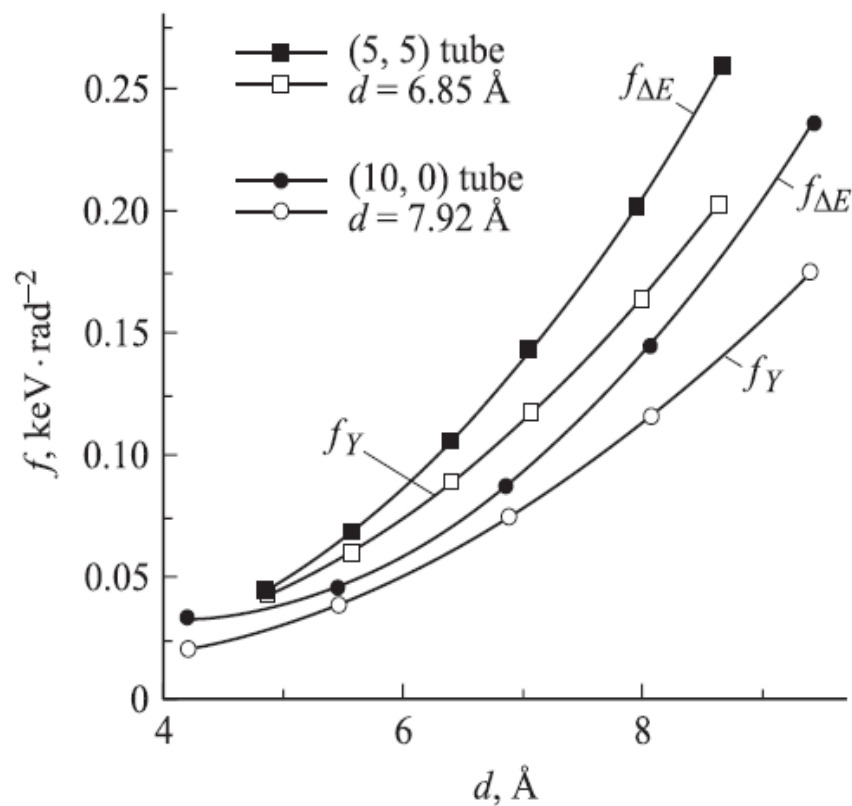
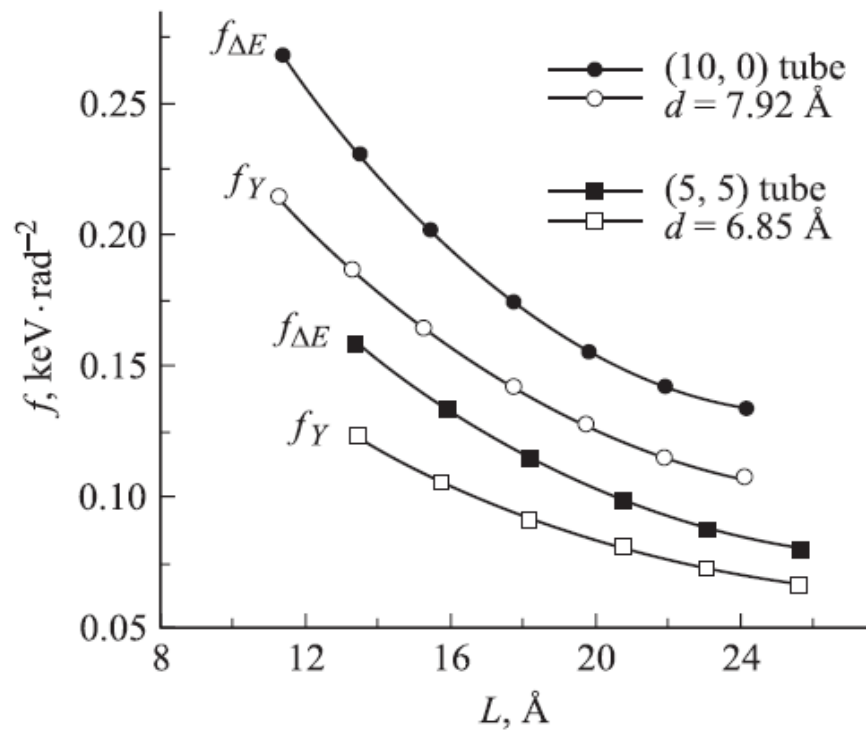
- 4) Calculation the Young's modulus for the elastic tension of nanoribbon on 1% on formula:

$$Y = \frac{F}{S} \frac{L}{\Delta L}$$

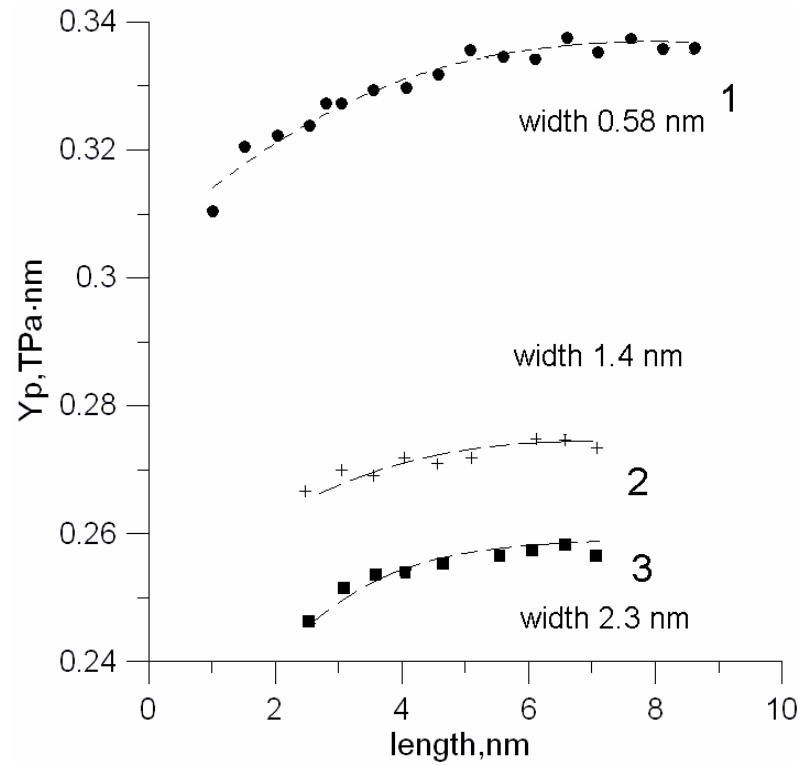
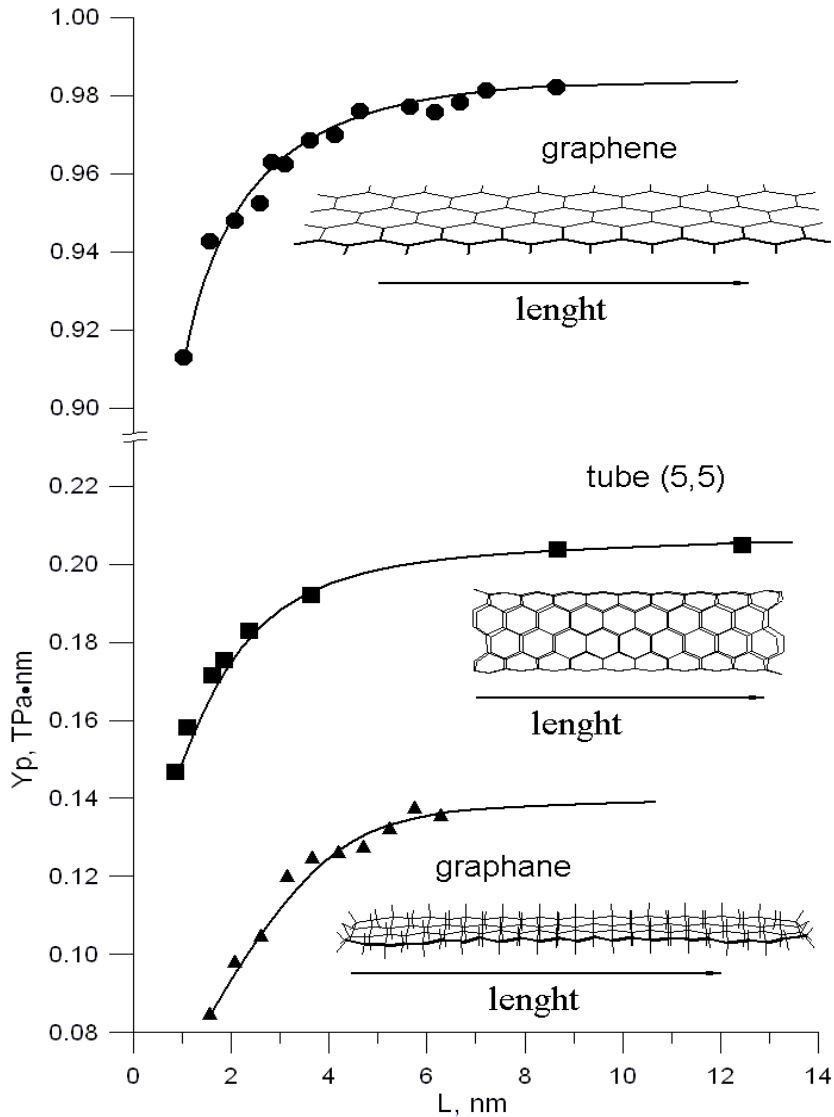
Young's pseudo-modulus (Y^{2D}) of nanotubes. $Y^{3D} = Y^{2D} * 0.34 \text{ nm}$

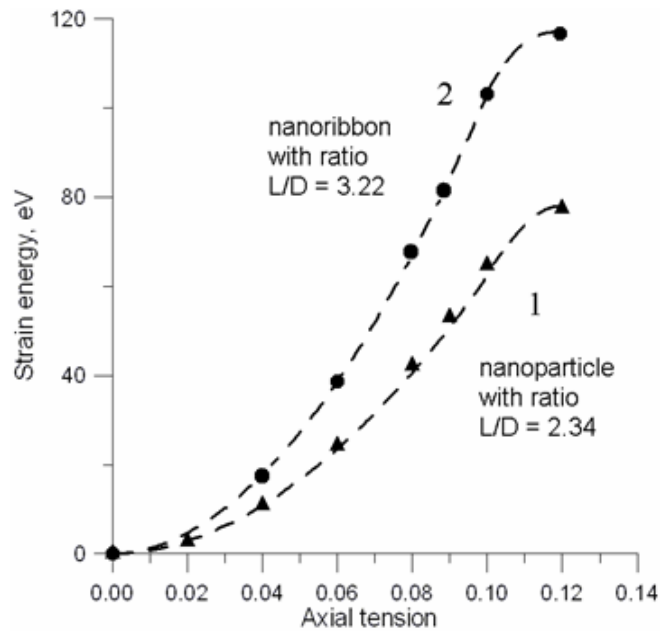


The torsion module CNT

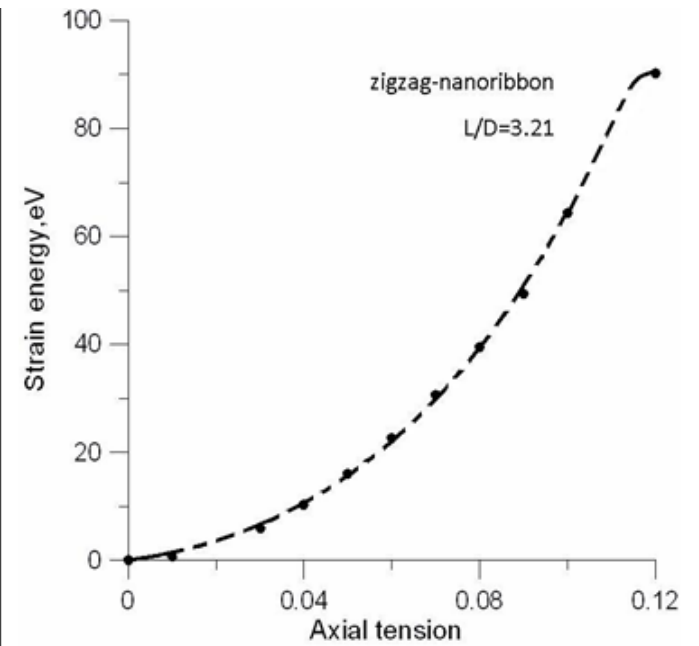


Young's pseudo-modulus (Y^{2D}) of nanoribbons. $Y^{3D} = Y^{2D} * 0.34 \text{ nm}$

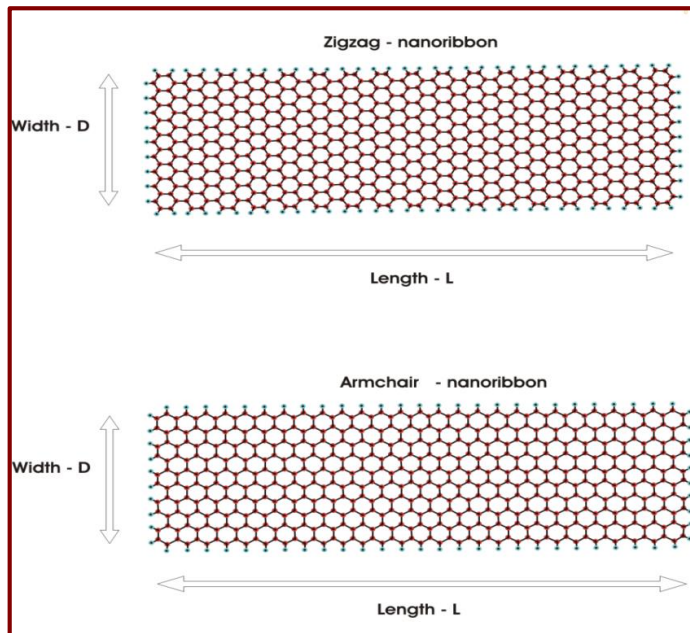




a) Armchair-nanoribbons



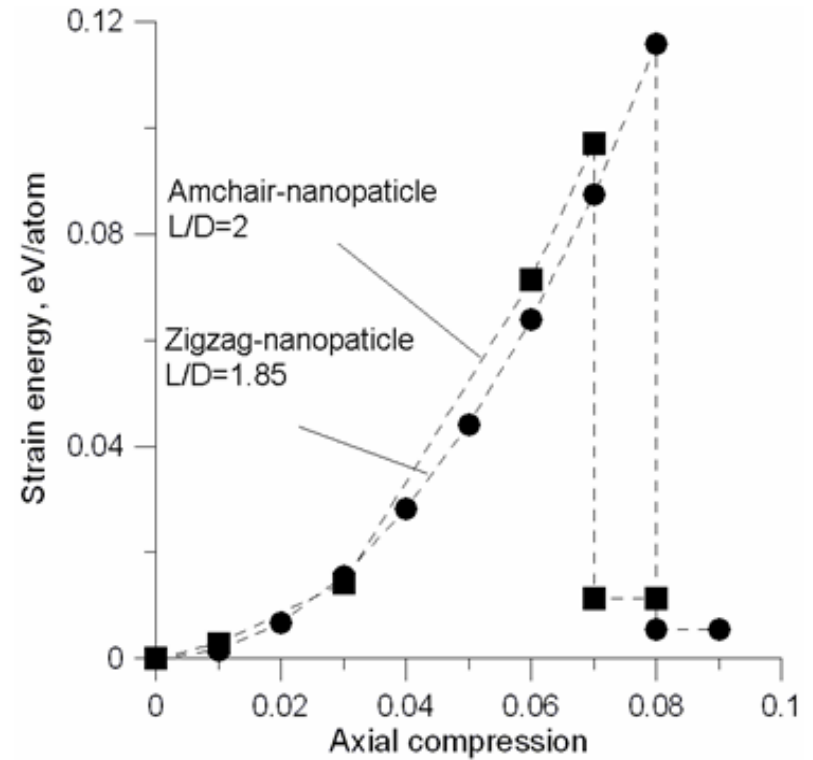
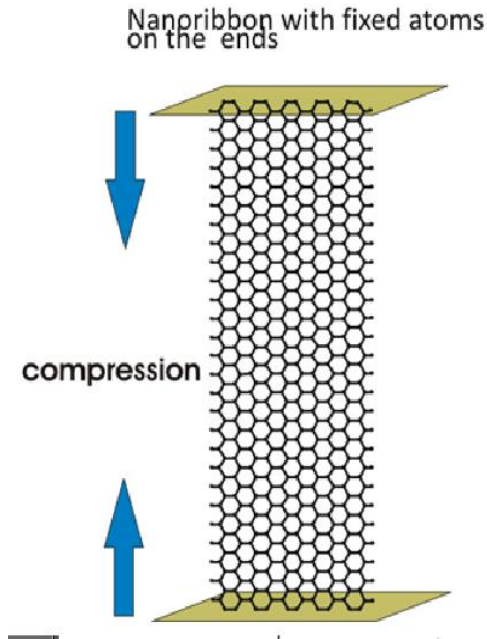
b) Zigzag-nanoribbons



Strain energy of nanoribbons undergoing axial tension

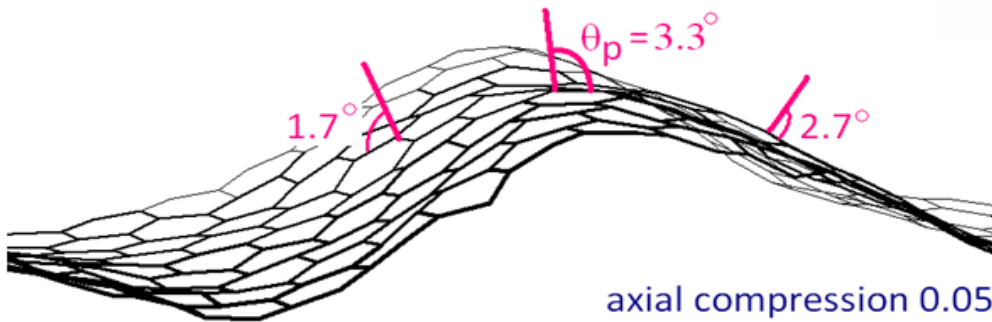
O.E. Glukhova, A.S. Kolesnikova // Physics of the Solid State (Springer). 2011. Vol. 53. No.9 P. 1957-1962.

Nanoribbon undergoing axial compression



pyramidalization angles

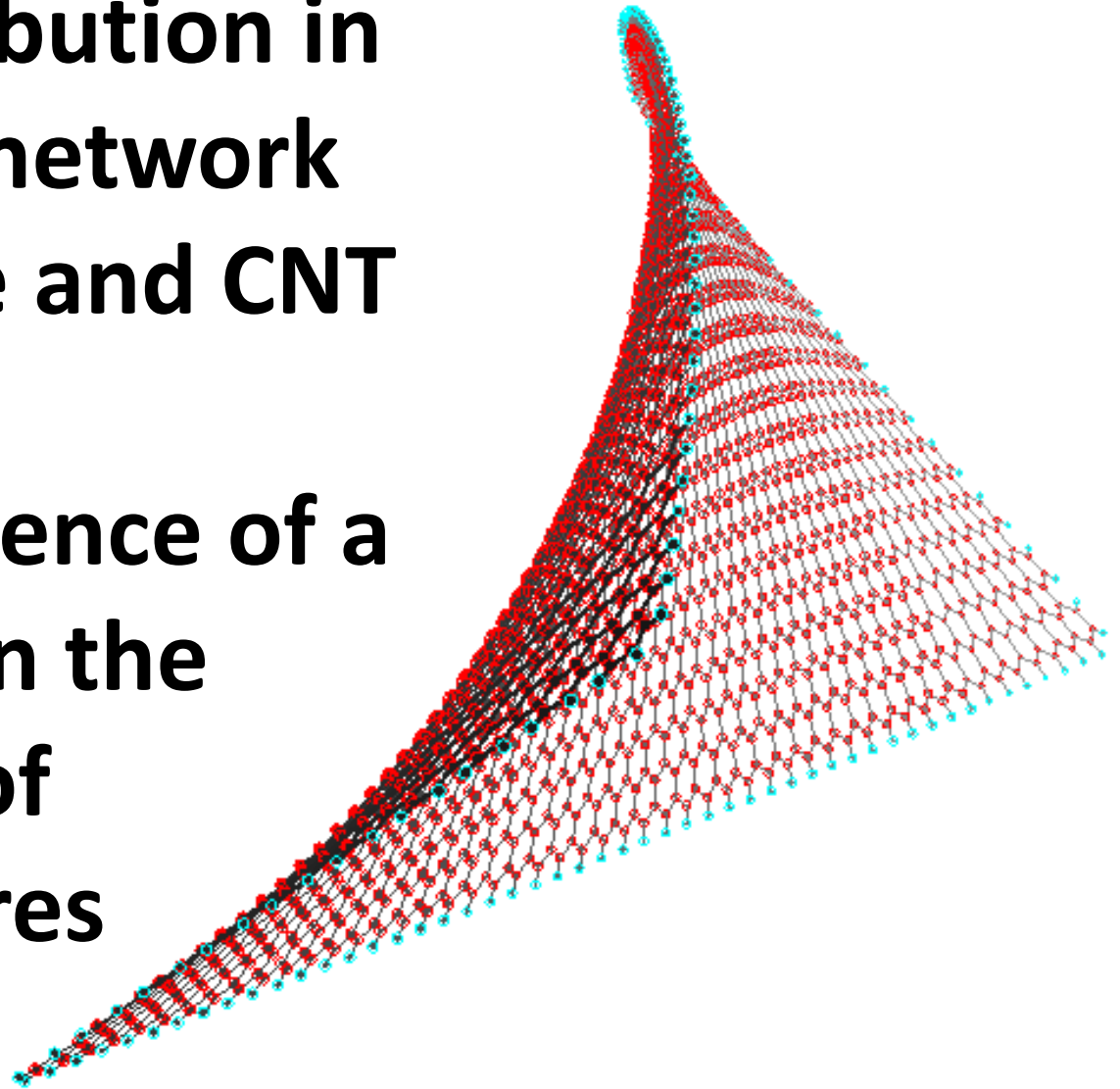
$$\theta_p = \theta_{\sigma\pi} - \pi/2$$



O.E. Glukhova, I.N.Saliy, R.Y.Zhnichkov, I.A.Khvatov, A.S.Kolesnikova and M.M.Slepchenkov
 // Journal of Physics: Conference Series 248 (2010) 012004

Stress distribution in the atomic network of graphene and CNT

IV. The influence of a curvature on the properties of nanostructures



The local stress field of the atomic grid of nanostructures: original method (Olga Glukhova and Michael Slepchenkov //Nanoscale, 2012, 4, 3335–3344)

It is proposed to carry out the calculation of the local stress field according to the following algorithm.

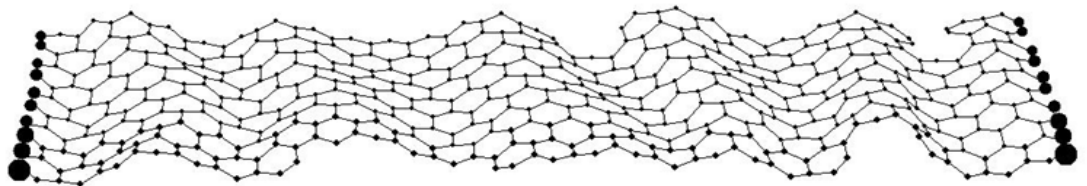
(1) Optimization of the initial structure by means of the quantum-chemical method.

(2) Calculation of distribution of the bulk energy density per atom using the empirical method.

(3) Search of the atomic configuration of the nanostructure subjected to the external influence as a result of the energy minimization for coordinates, using the quantum-chemical method.

(4) Calculation of the distribution of the bulk energy density per atom in the structure subjected to the external influence, using the empirical method.

(5) Calculation of the local stress in the atomic grid according to the difference between the values of the bulk density of energy for the atoms of the structure subjected to the external influence, and the initial structure.



The bulk energy density w_i of the atom i was calculated by the formula:

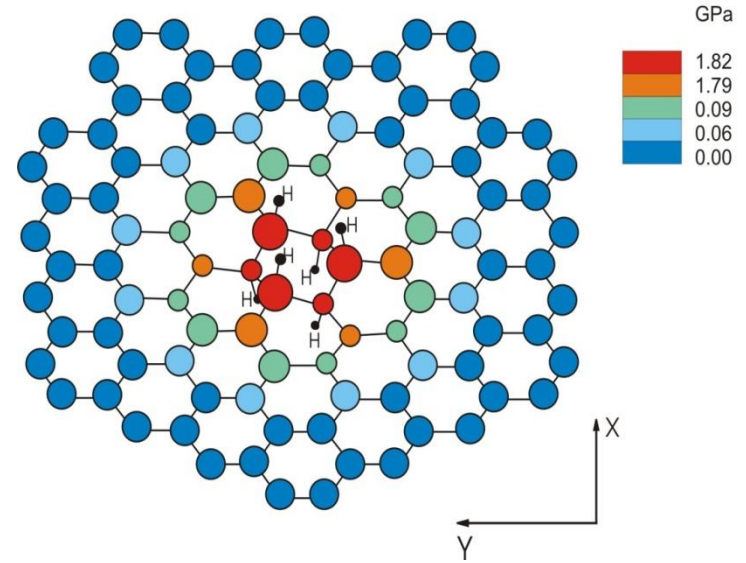
$$w_i = \left(\sum_{j(\neq i)} (V_R(r_{ij}) - B_{ij}V_A(r_{ij})) + \sum_{j \neq i} \left(\sum_{k \neq ij} \left(\sum_{l \neq i,j,k} V_{\text{tros}}(\omega_{ijkl}) \right) \right) + \sum_{j(\neq i)} V_{\text{vdW}}(r_{ij}) \right) / V_i$$

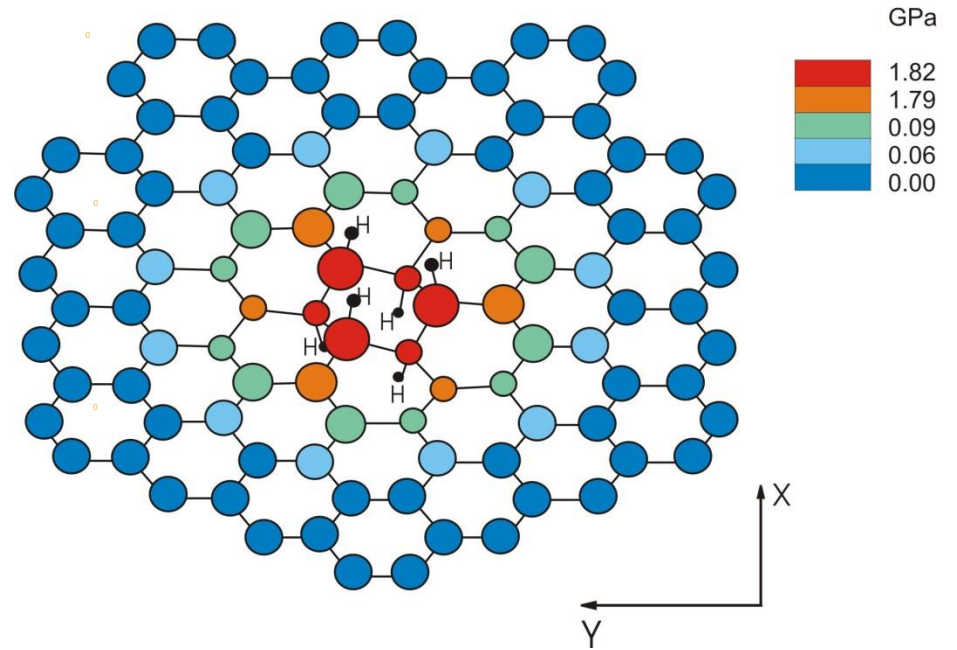
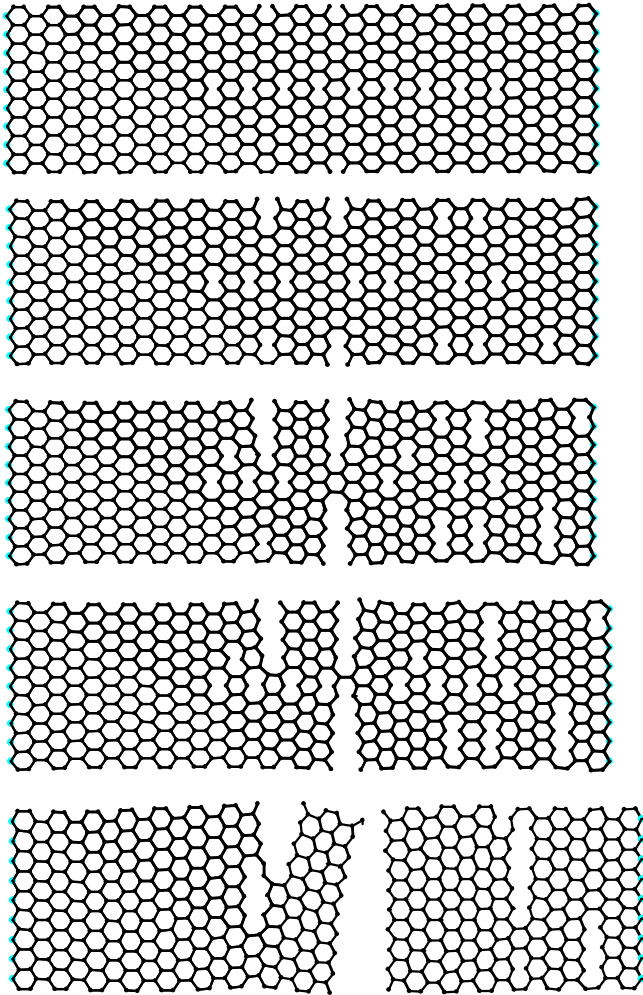
$$V_i = \frac{4}{3} \pi r_0^3$$

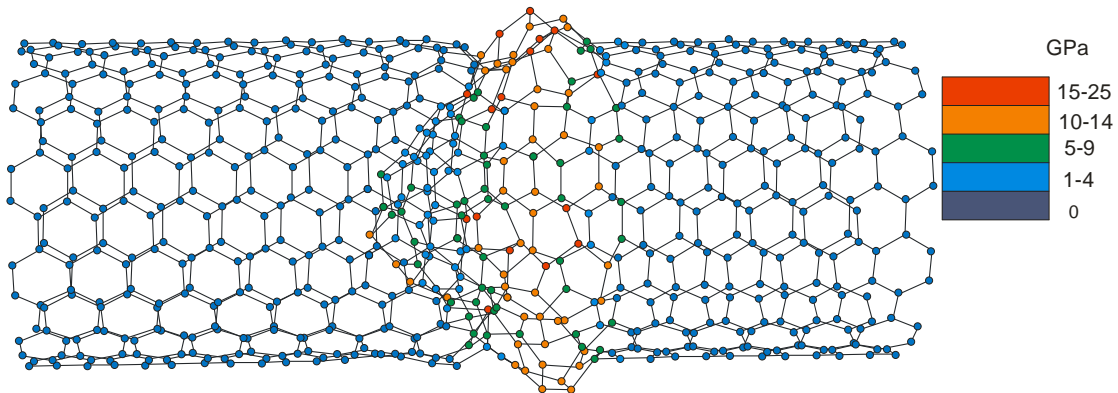
The stress of the atomic grid near the atom with number i is calculated as:

$$\sigma_i = |w_i - w_i^0|$$

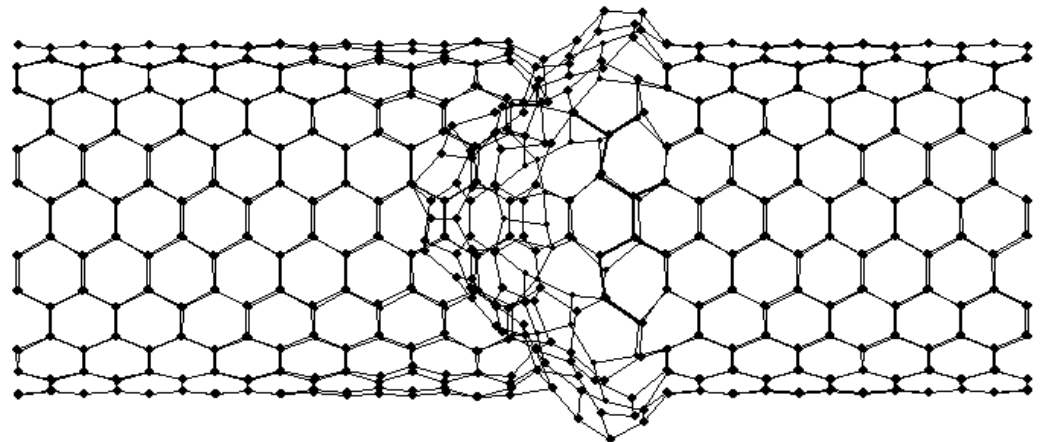
where w_i^0 is the bulk energy density of the i^{th} atom of the graphene sheet which is in equilibrium; w_i is the bulk energy density of an atom of the graphene sheet subjected to the external influence (deformation, defect formation, *etc.*). The value of w_i^0 in the centre of the graphene sheet is equal to -58.60 GPa. At the edges of the graphene sheet the bulk energy density is higher since the atoms of the edges have only two links with other carbon atoms. It is equal to -41.54 GPa on an armchair edge and on the zigzag edge is equal to -40.64 GPa. It is suggested that without an external influence the stress equals to zero for the atoms in the centre and at the edges of the graphene sheet.



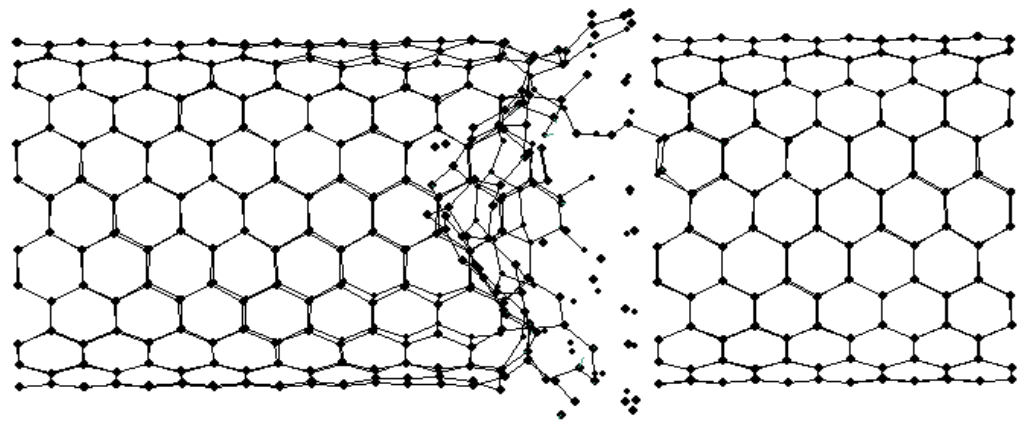


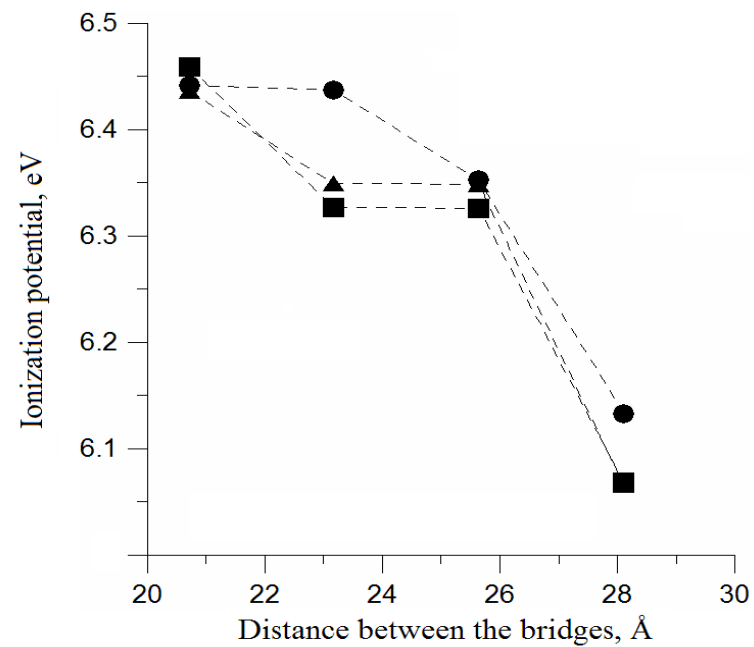
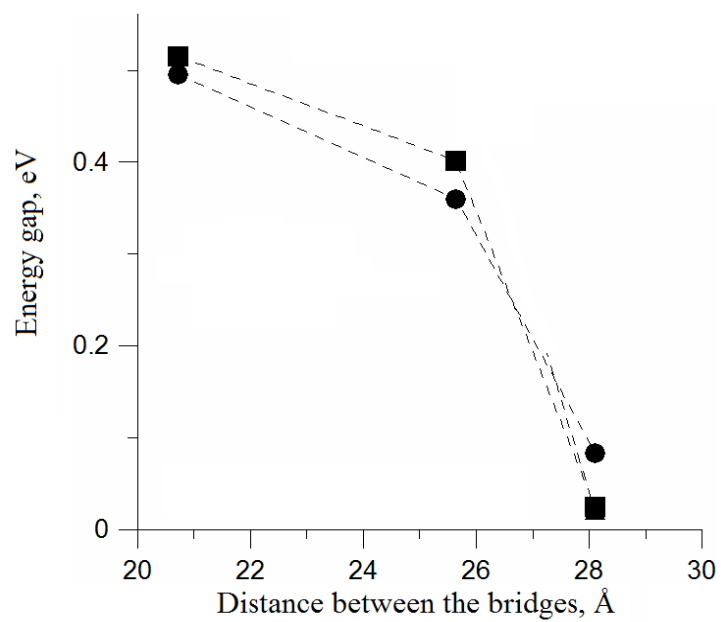
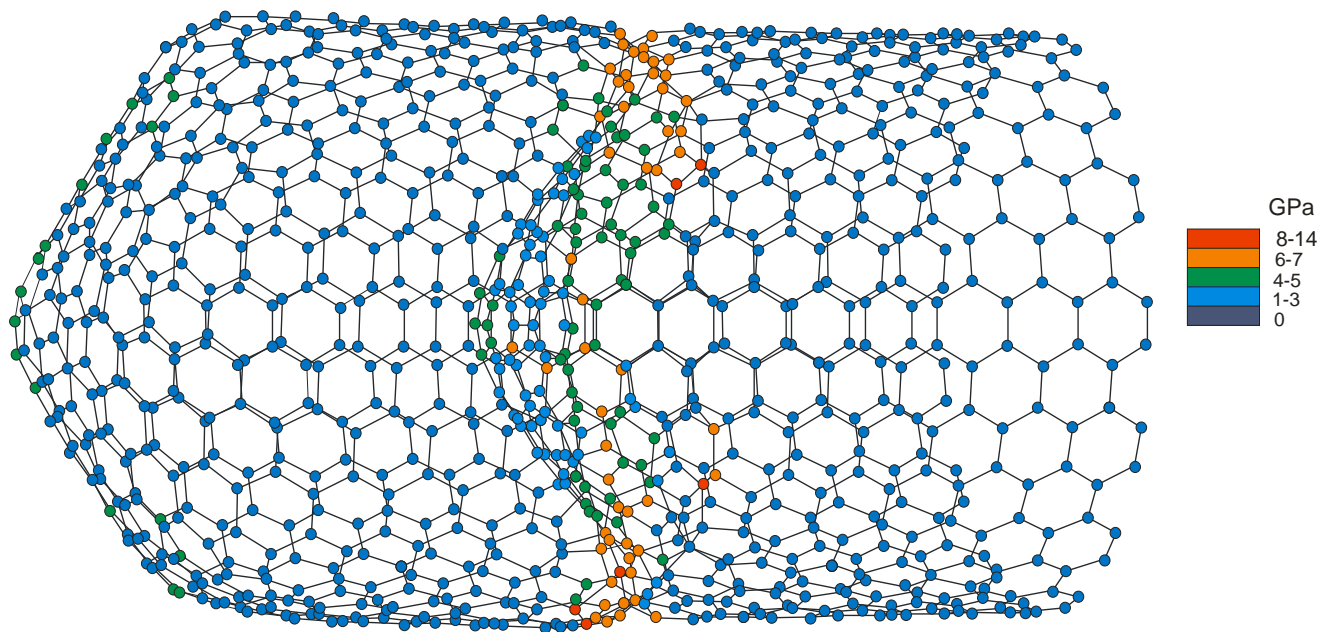


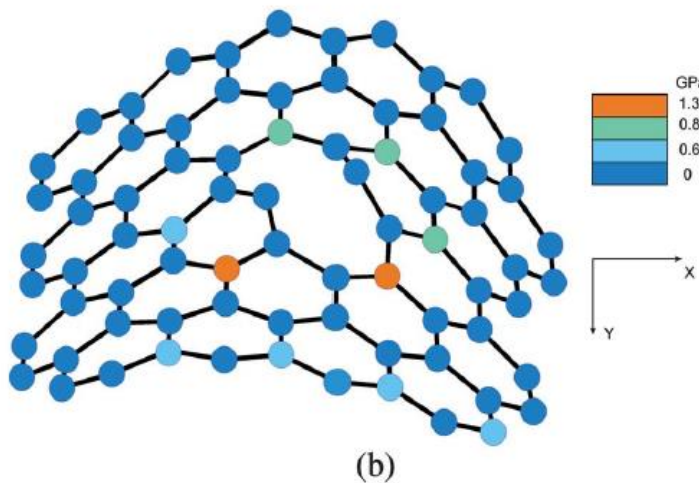
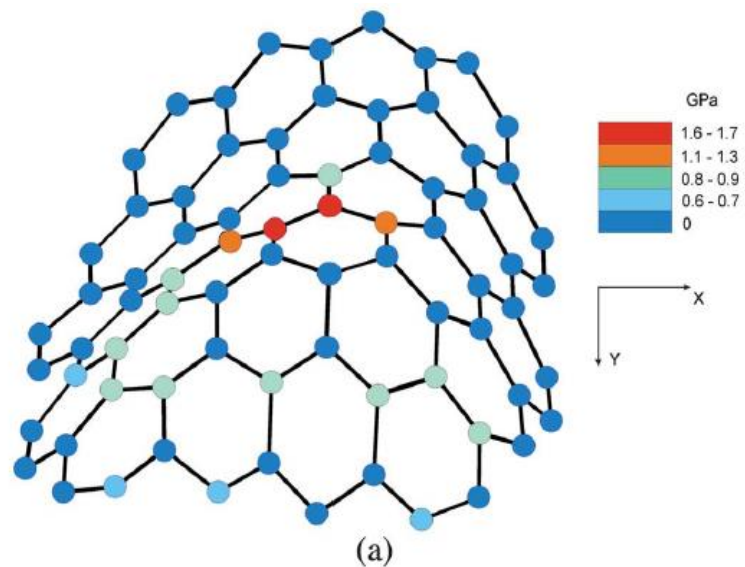
Destruction of the structure of bamboo-like CNT during the increase of the temperature



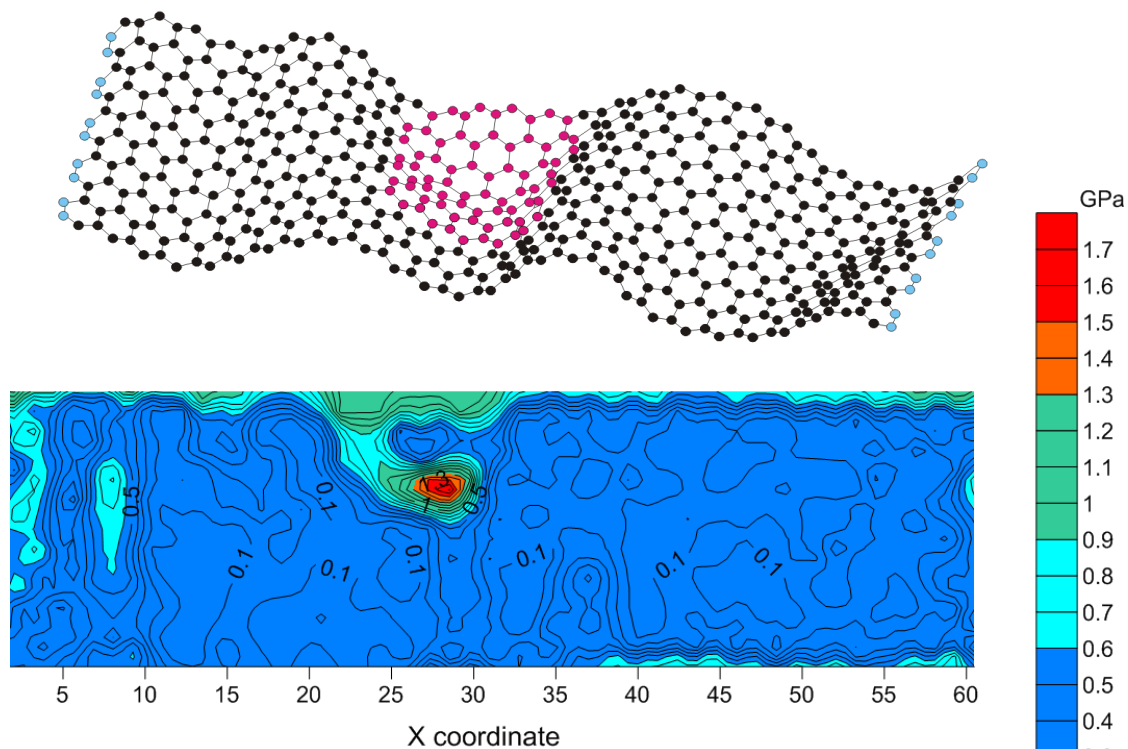
**O.E. Glukhova, I.V. Kirillova,
A.S. Kolesnikova, E.L. Kossovich,
G.N. Ten // Proc. of SPIE. 2012. Vol.
8233. P. 82331E-1-82331E-7.**





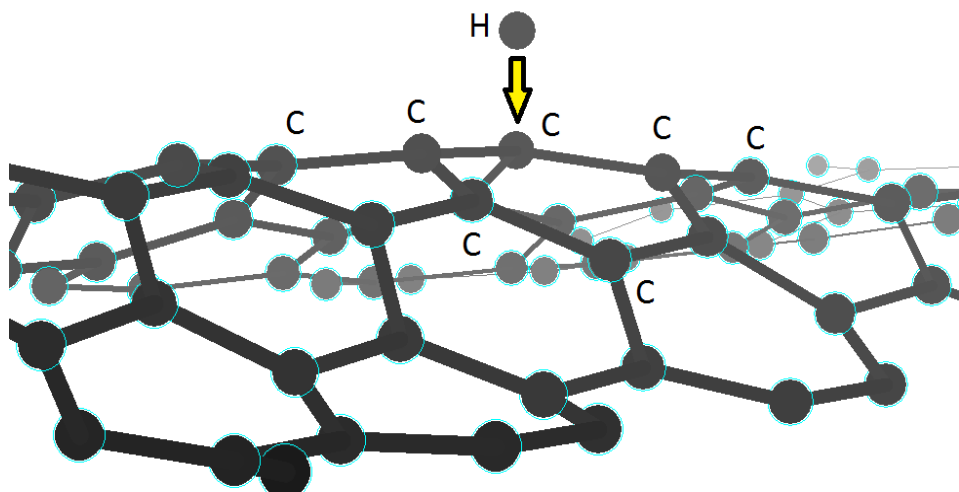


Prediction of the defects appearance

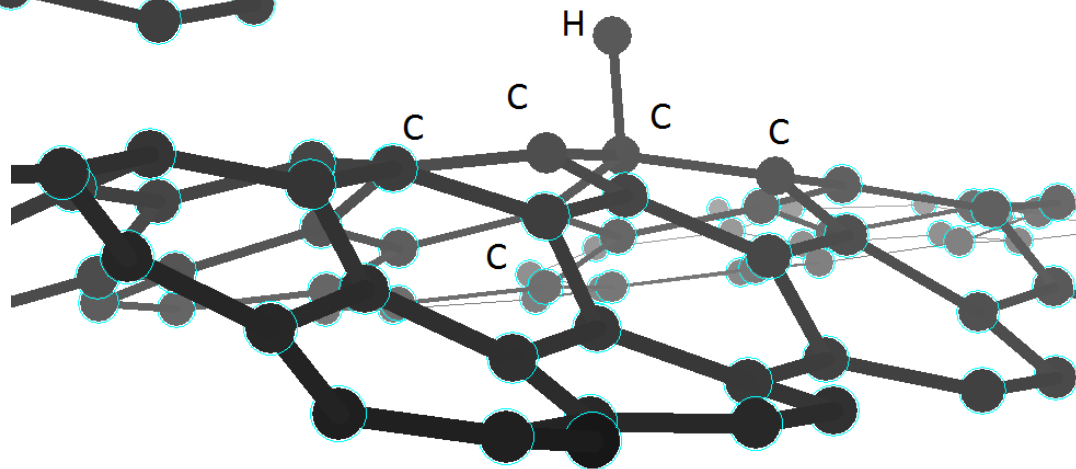


Defects of the C–C bond are observed only between atoms with a local stress value of about 1.8 GPa. One of the most stressed sections of the atomic grid containing a defect is presented in Fig. 4. From the Figure it is clearly seen that after C–C-bond breaking the atomic grid reconstructs and the stress decreases. The enthalpy of the defect formation equals $163.5 \text{ kcal mol}^{-1}$.

The influence of a curvature on the properties of nanostructures



The absorption of H-atom on the atomic network

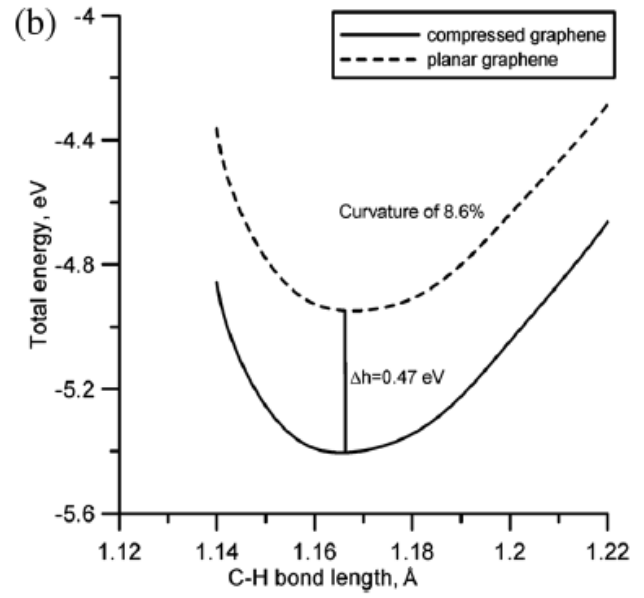
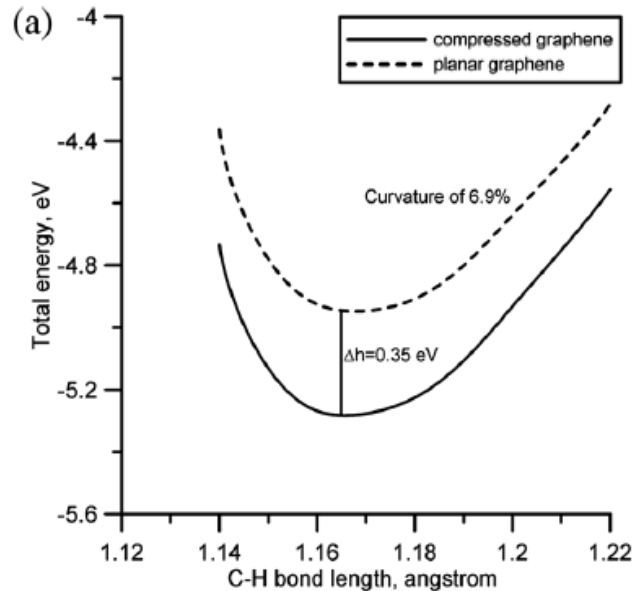
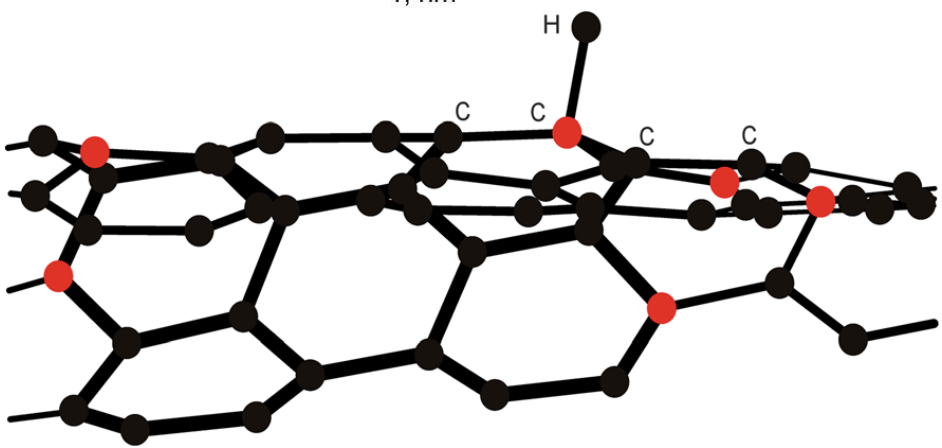
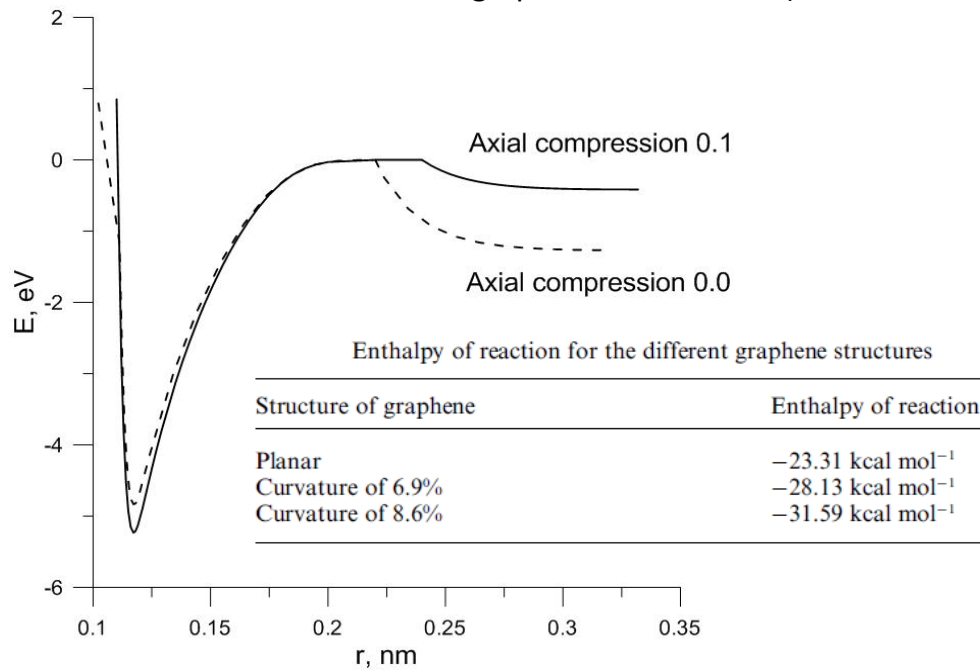


O.E. Glukhova, I.V. Kirillova, M.M. Slepchenkov The curvature influence of the graphene nanoribbon on its sensory properties // Proc. of SPIE. 2012. Vol. 8233. P. 82331B-1-82331B-6.

Olga E. Glukhova, Michael M. Slepchenkov Influence of the curvature of deformed graphene nanoribbons on their electronic and adsorptive properties: theoretical investigation based on the analysis of the local stress field for an atomic grid // Nanoscale 2012. Issue 11. Pages 3335-3344. DOI:10.1039/C2NR30477E.

The total energy of the structure depends on the distance between the hydrogen atom and the carbon atom.

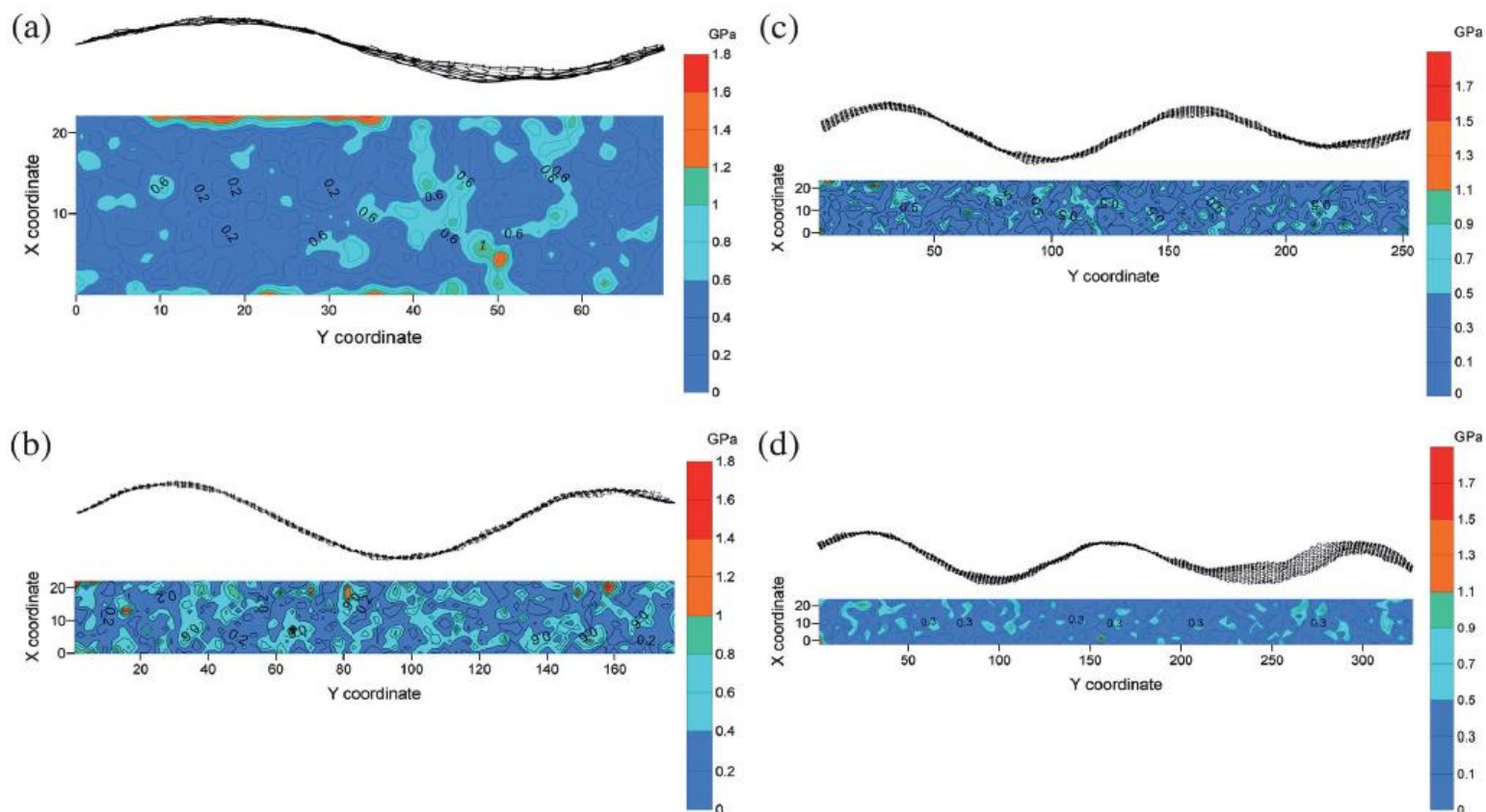
(The dashed line is the interaction of the hydrogen atom with planer graphene nanoribbon; the solid line is the interaction of the hydrogen atom from wave-like graphene nanoribbon)



The dependence of the chemical C–H interaction energy on the length of the C–H bond for the planar and compressed graphene nanoribbon: (a) with curvature of 6.9%; (b) with curvature of 8.6%.

Geometrical characteristics of the curved armchair graphene nanoribbons compressed up to 98% of initial length

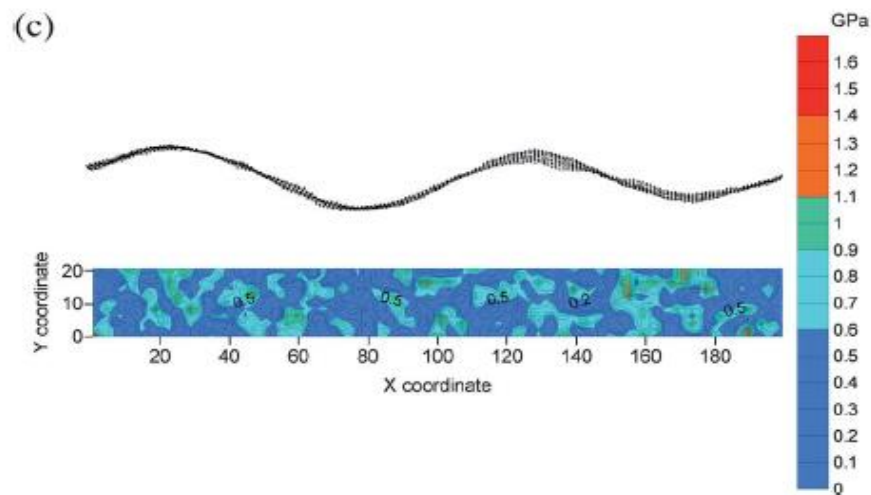
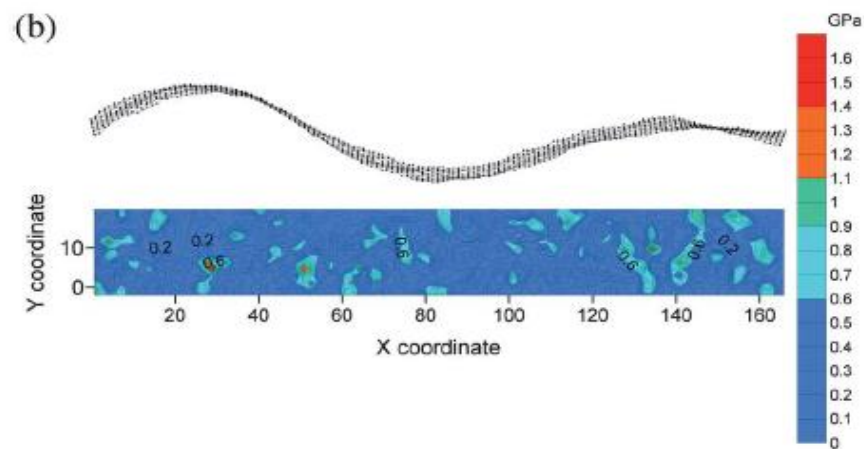
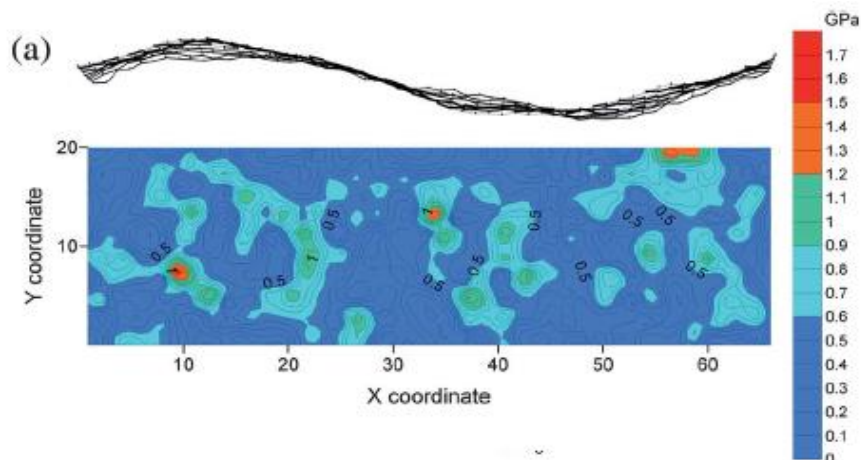
Number of half-waves	Number of atoms in structure	Length of nanoribbon/Å	Length of half-wave/Å	Amplitude of half-wave/Å	Number of hexagons in half-wave	Width of nanoribbon/Å
2	646	71.0	35.5	2.2	9	22.4
3	1634	181.7	60.5	5.3	14	22.4
4	2318	258.4	64.6	5.65	15	22.4
5	3002	335.12	66.2	5.4	15	22.4



Map of distribution of the local stress for the nanoribbon armchair: (a) in the case of two half-waves; (b) in the case of three half-waves; (c) in the case of four half-waves; (d) in the case of five half-waves.

Geometrical characteristics of the curved zigzag graphene nanoribbons compressed up to 98% of the initial length

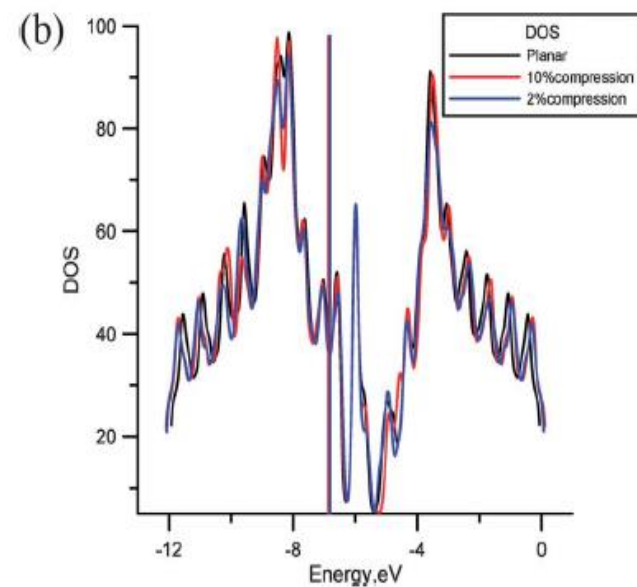
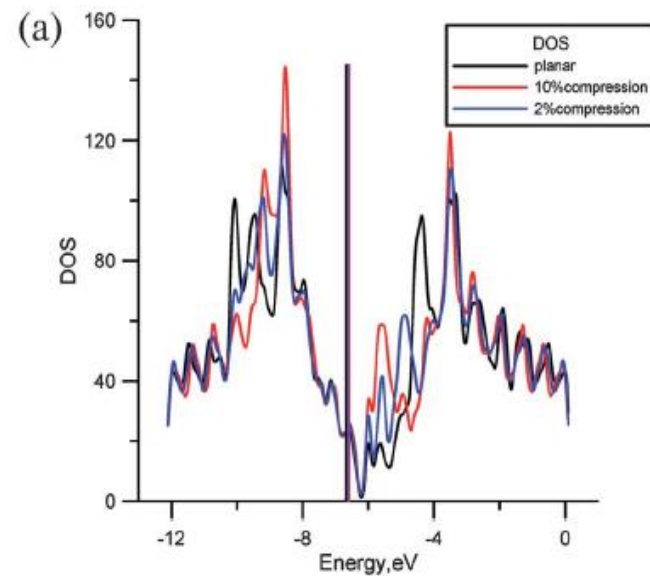
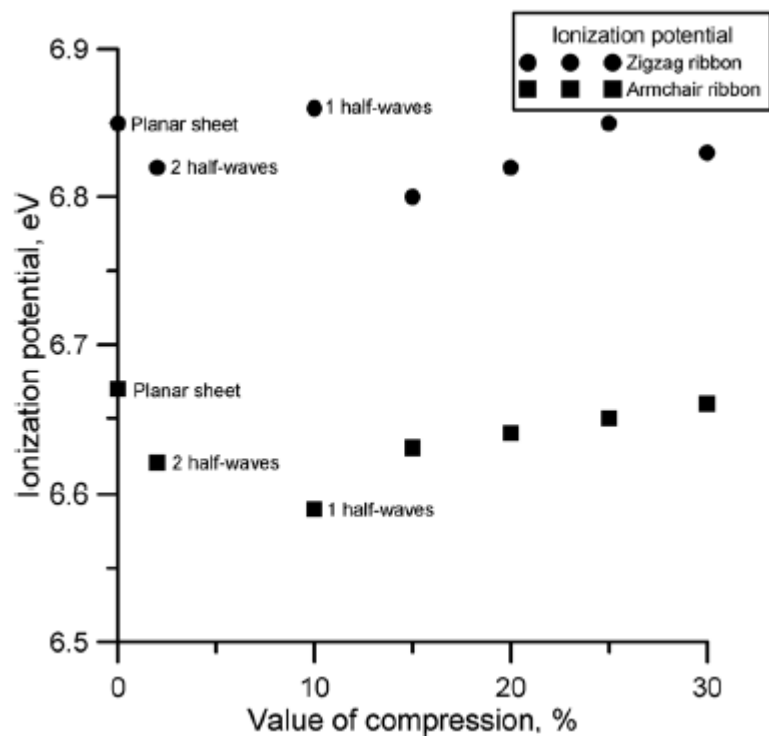
Number of half-waves	Number of atoms in structure	Length of nanoribbon/Å	Length of half-wave/Å	Amplitude of half-wave/Å	Number of hexagons in half-wave	Width of nanoribbon/Å
2	550	65	32.5	2.8	12	19.88
3	1390	165.18	55.06	5.4	20	
4	1670	198.7	49.6	5.6	20	



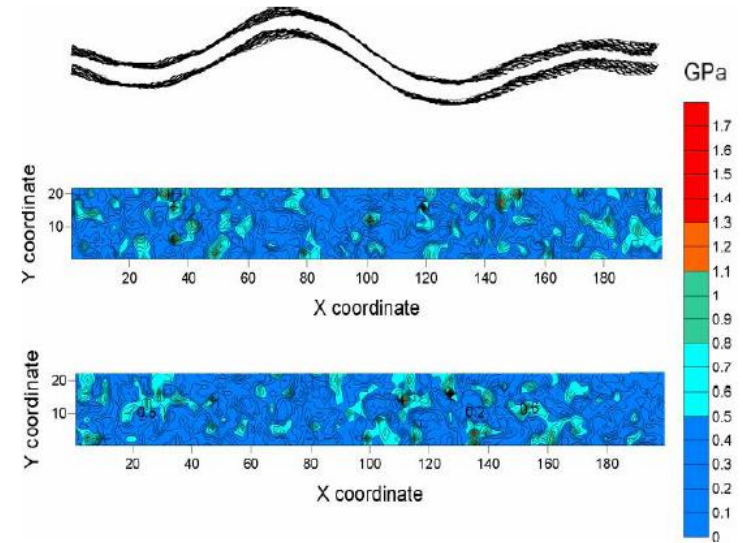
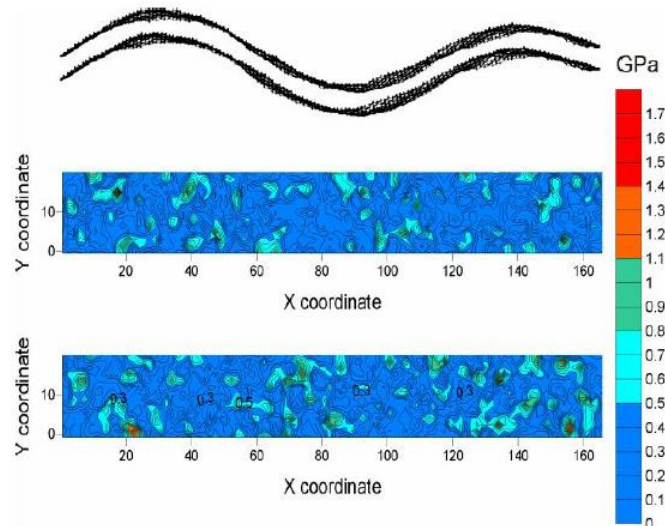
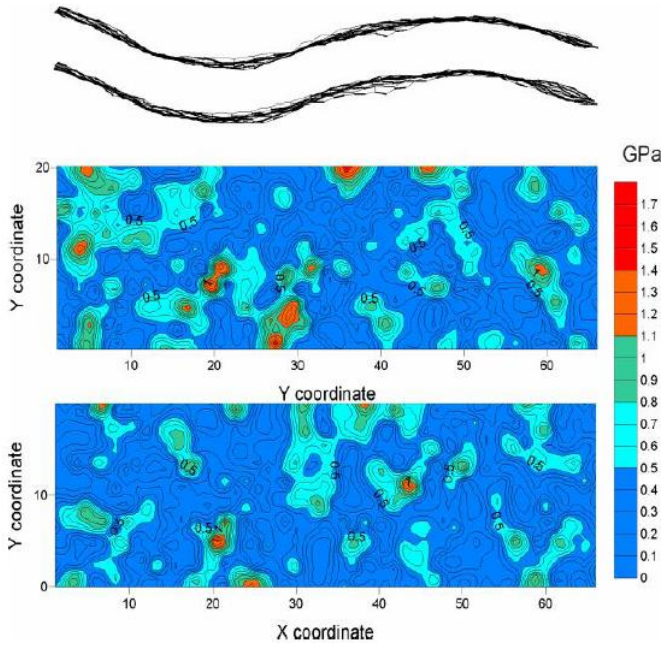
Map of distribution of the local stress for nanoribbon zigzag: (a) in the case of two half-waves; (b) in the case of three half-waves; (c) in the case of four half-waves.

Some parameters of the electronic structure of nanoribbons

Number of half-waves	Length of half-wave/ \AA	IP/eV	E_{gap}/eV
<i>Armchair ribbon of width 22.4 \AA</i>			
2	71.0	6.63 (6.65)	0.04 (0.03)
3	181.7	6.50 (6.53)	0.04 (0.03)
4	258.4	6.44 (6.47)	0.02 (0.01)
5	335.12	6.41 (6.44)	0.04 (0.02)
<i>Zigzag ribbon of width 19.88 \AA</i>			
2	65	6.82 (6.84)	0.04 (0.02)
3	165.18	6.79 (6.81)	0.01 (0.01)
4	198.7	6.80 (6.81)	0.01 (0.01)



The compression process of bi-layer graphene



Geometrical characteristics of the curved zigzag bi-layer graphene nanoribbons compressed up to 98% of the initial length

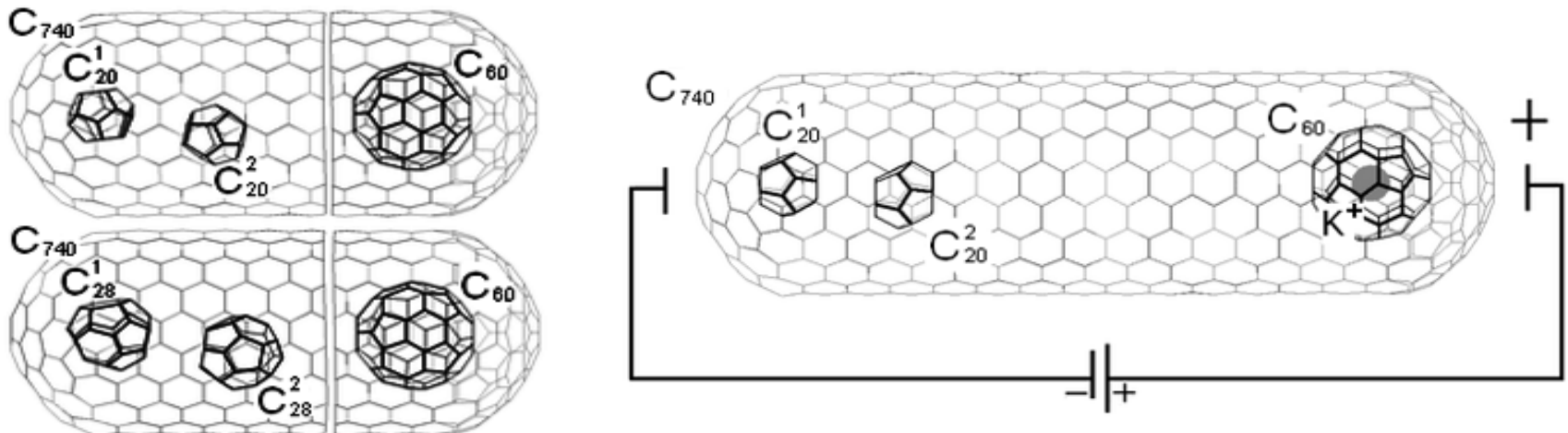
Num ber of half- wave s	Num- ber of atoms in struc- ture	Length of nanorib- bon, Å	Leng- th of half- wav- e, Å	Ampli- tude of half- wave, Å	Num- ber of hex- agons in half- wave	Width of nanorib- bon, Å
2	1100	65	32.3	3.1	13	
3	2780	165.18	55.4	5.48	20	19.88
4	3340	198.7	49.8	5.55	20	

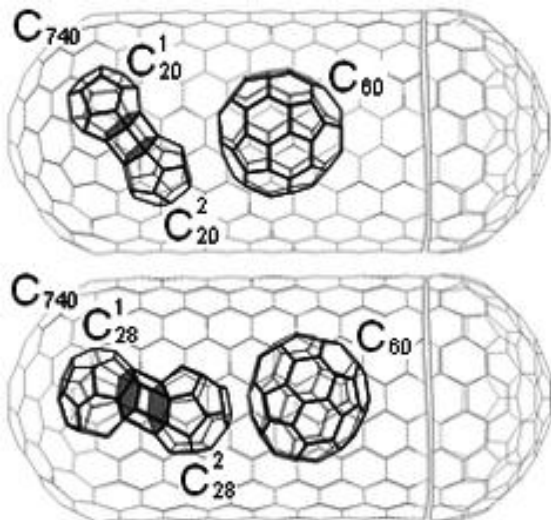
NANODEVICES

Nanoreactor (nanoautoclave)

Dimerization of miniature C_{20} and C_{28} fullerenes in nanoautoclave
(Olga E. Glukhova // Journal of Molecular Modeling, Volume 17, Issue 3
(2011), Page 573)

In our nanoautoclave model a closed single-wall carbon nanotube (10,10) C_{740} is represented as a capsule that is closed from both ends with C_{240} fullerene caps. The pressure is controlled by a shuttle-molecule encapsulated into a nanotube that may move inside the tube. In the present case a shuttle-molecule is the C_{60} fullerene. The shuttle must have some electric charge for its movement to be controlled by an external electric field. The positively charged endohedral complex $K^+@C_{60}$ (the ion of potassium inside the fullerene C_{60}) is a shuttle-molecule in the present model of the nanoautoclave. So, the hybrid compound $K^+@C_{60}@tubeC_{740}$ is a nanoautoclave model. The $K^+@C_{60}@tubeC_{740}$ nanoparticle is located between two electrodes connected with a power source. Changing the potentials at the electrodes, we control the movement of the $K^+@C_{60}$





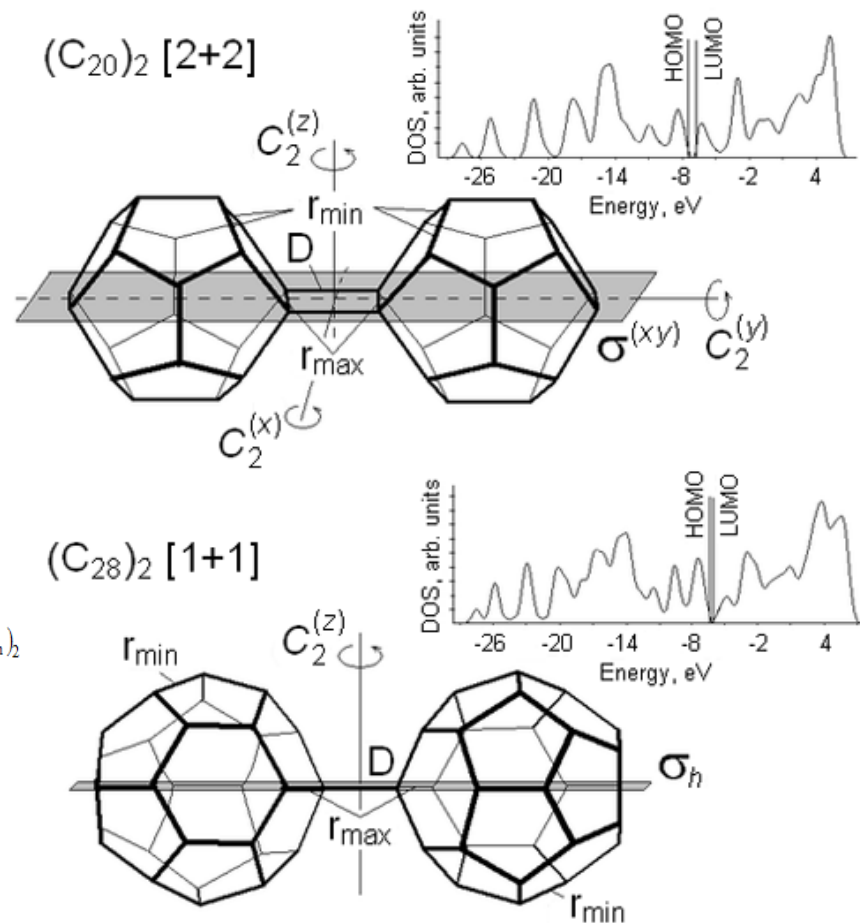
When the pressure created in the tube provides both the overlap of π -electrons of the C_n fullerenes (that corresponds to the interatomic distance of about 1.9 Å) and the covalent bonds formation, the intermediate phase of the $(C_n)_2$ dimer is synthesized: $(C_{20})_2 [5+5]$ (at $n = 20$) or $(C_{28})_2 [6+6]$ (at $n = 28$). Here a number of fullerene atoms participating in the intermolecular bonds formation is shown in square brackets. Figure shows a stable dimer of the C_{20} (C_{28}) fullerene and the C_{60} molecule that suffered a certain deformation.

Characteristics of stable fullerenes dimers

Dimer	Symmetry group of the dimer	r_{\min}/r_{\max} , Å	D , Å	E_b , eV	ΔH , kcal/mol·atom	E_g , eV	HOMO, eV
$(C_{20})_2 [2+2]$	D_{2h}	1.43/1.62	1.65	6.44	-5.01	0.66	7.00
$(C_{28})_2 [1+1]$	C_{2h}	1.41/1.56	1.56	6.57	-2.07	0.14	7.16

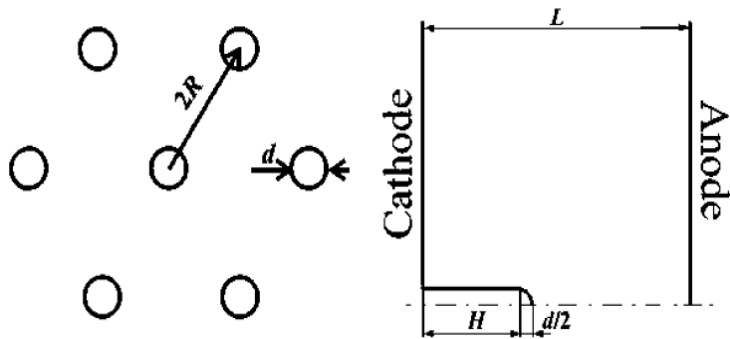
The energy of the C_{60} fullerene and parameters of the outer field necessary for the $(C_n)_2$ dimer synthesis

$(C_n)_2$	$E_{inter}(t)$, eV	ΔE_{inter} , eV	$\Delta\phi$, V	F , V/m
$(C_{20})_2 [2+2]$	-3.574	5.42	8.90	$0.18 \cdot 10^8$
$(C_{28})_2 [1+1]$	-3.574	6.50	10.16	$2 \cdot 10^8$

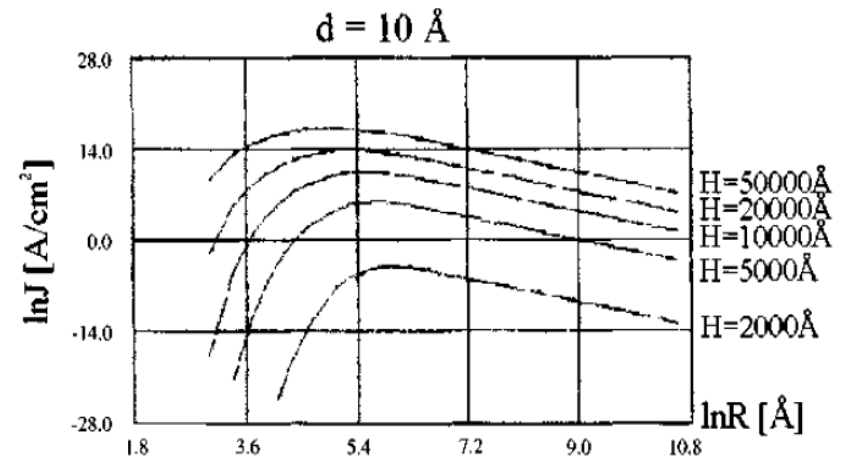
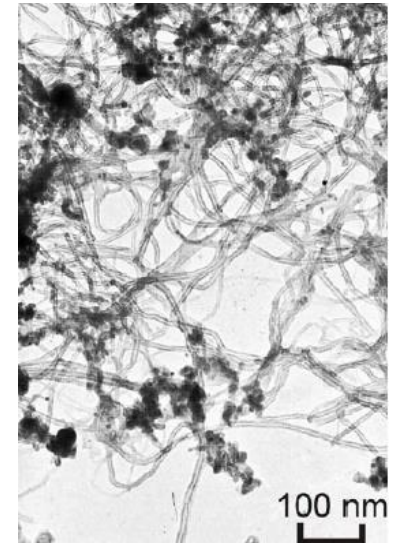
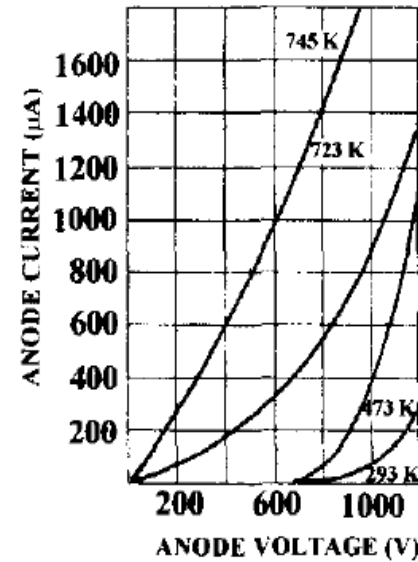
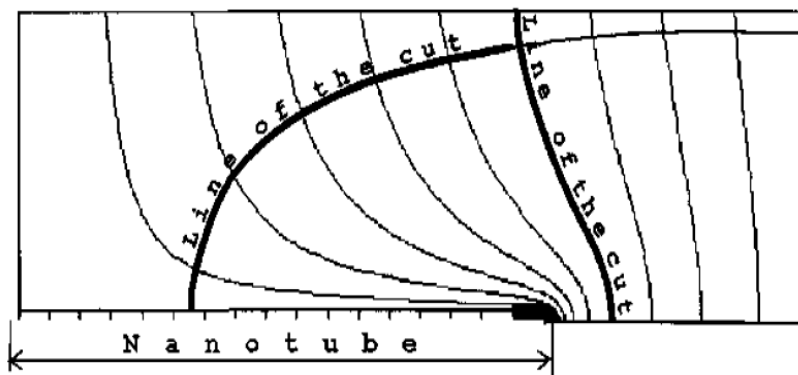


Carbon nanotubes are as emitters

N.I. Sinitsyn, Yu.V. Gulyaev, O.E. Glukhova et al. // Applied Surface Science, 1997. V.11. P.145-150.

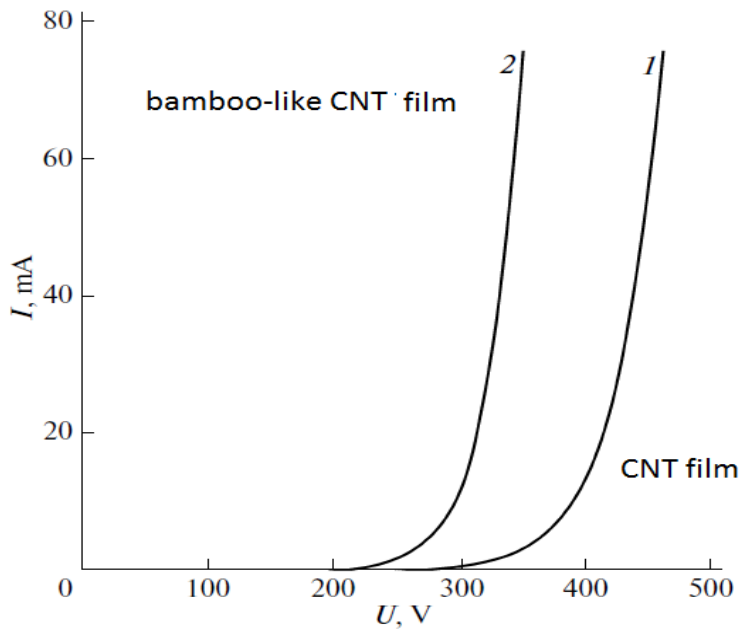


Scheme of the computational model of aligned nanotube film.



O.E. Glukhova, A.I.Zhbanov, G.V.Torgashov et al. // Applied Surface Science, 2003. V.215 (Issue 1-4) 15 June. P.149-159
 N.I. Sinitsyn, Yu.V.Gulyaev, O.E. Glukhova et al. // J. Vac. Sci. Technol. B 15(2), Mart/Apr 1997. P. 422-424.

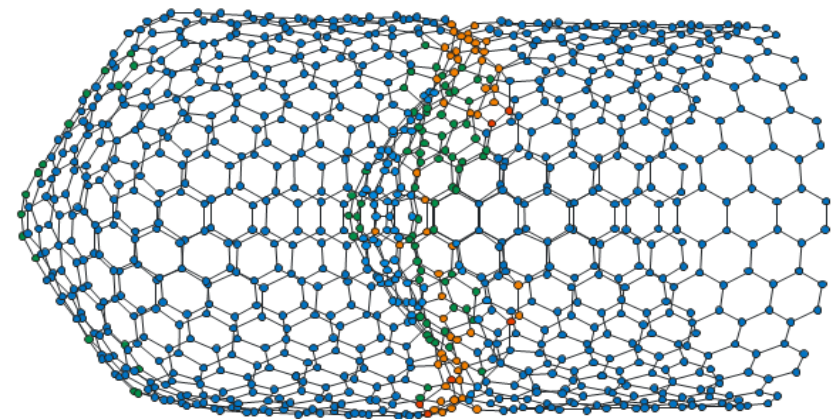
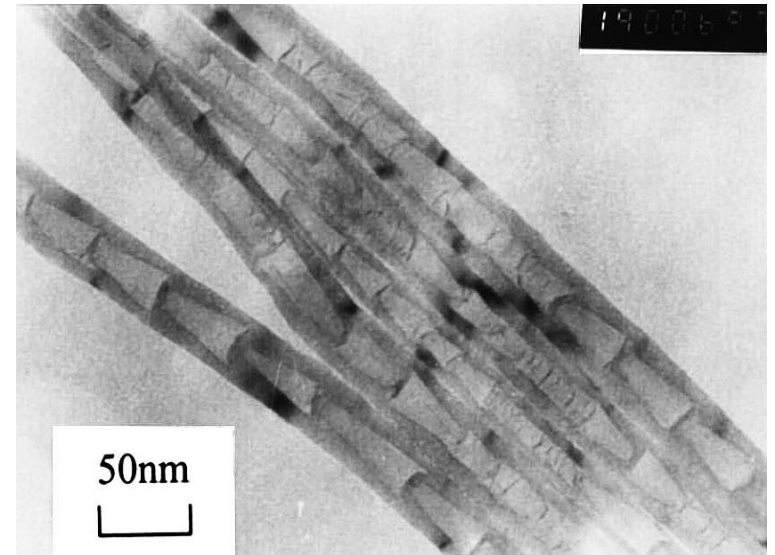
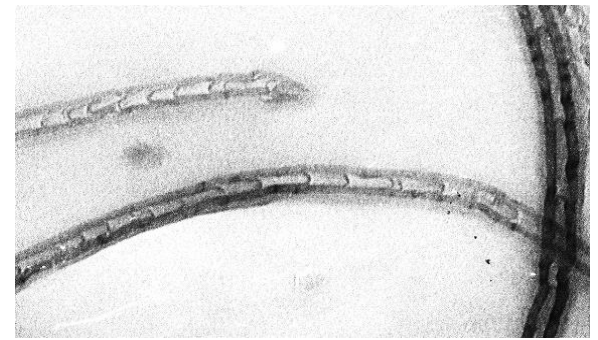
The Institute of
Radioengineering
and Electronics
(IRE) of
Russian Academy
of Sciences



Current–voltage characteristics

Characteristics of the bamboo-shaped (10, 10) nanotubes

Number of compartments	R , nm	L , nm	Y , TPa	f , keV rad ⁻²
0	0.674	4.051	2.251	0.298
1	0.674	3.772	2.593	0.306
2	0.674	3.752	2.710	0.454
3	0.674	3.961	2.862	0.535



*O.E. Glukhova, A.S. Kolesnikova, G.V. Torgashov,
Z.I. Buyanova // Physics of the Solid State (Springer),
2010, Vol. 52, No. 6, pp. 1323–1328.*

Effect of Bending on the Polymerization of Fullerenes Inside Carbon Nanotubes

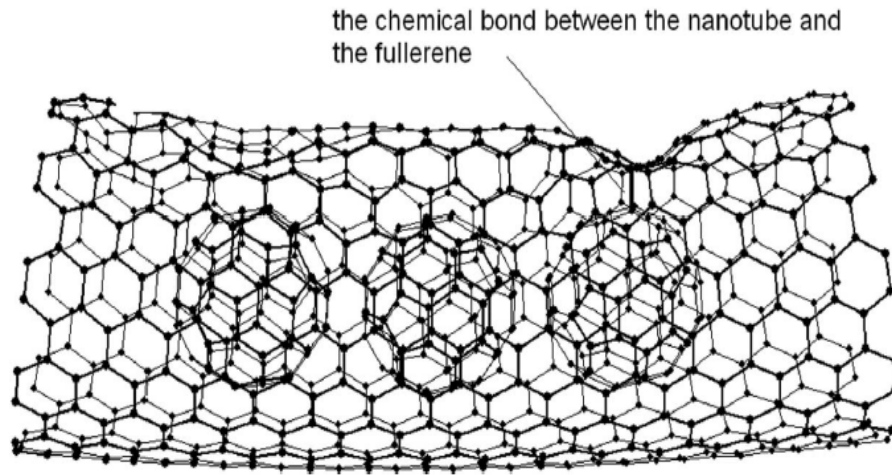
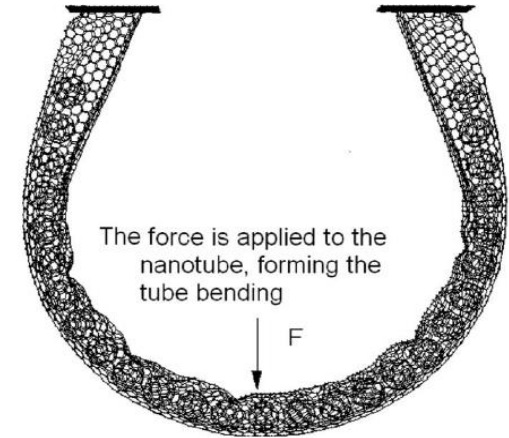


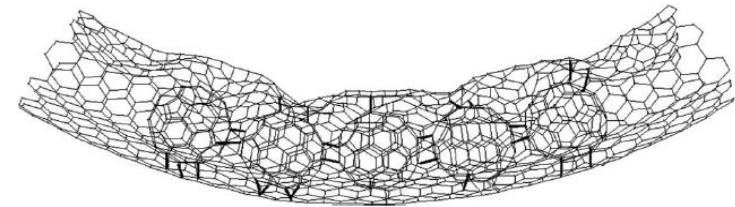
Figure 3. Fragment of peapod at bending 16 degrees.

It can be concluded that by bending the peapod 270 degrees the phase transition occurred, accompanied by the formation of the new curved structure. It was established that at such a bending:

1. The atomic structure of peapod is not destroyed.
2. The nanotubes surface of smaller radius becomes wave-like and, in some places of trough, is connected with the fullerenes.
3. The fullerenes come to the distance of 0.14 nm between the atoms of the cell and are polymerized.
4. The hybrid compound of the nanotube which was formed retains the atomic structure unchanged even when there is no external load.
5. The minimum angle of the bending for the polymerization process is 16 degrees.



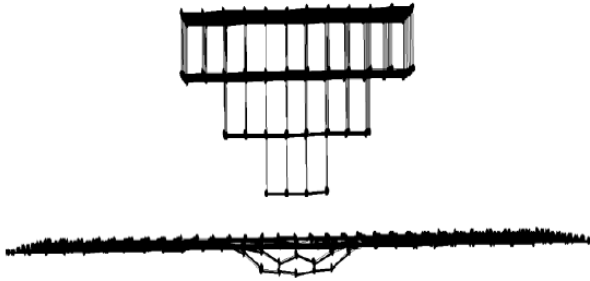
The peapod bending 270 degrees.



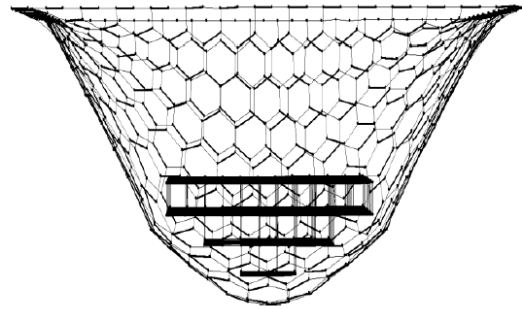
Fragment of peapod at bending 270 degrees.

The thick lines show the connections formed during the polymerization of fullerenes with neighboring fullerenes and a nanotube.

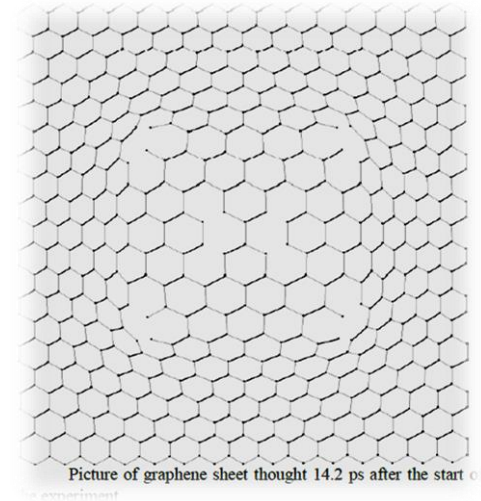
Investigation of the one-layer graphene plate



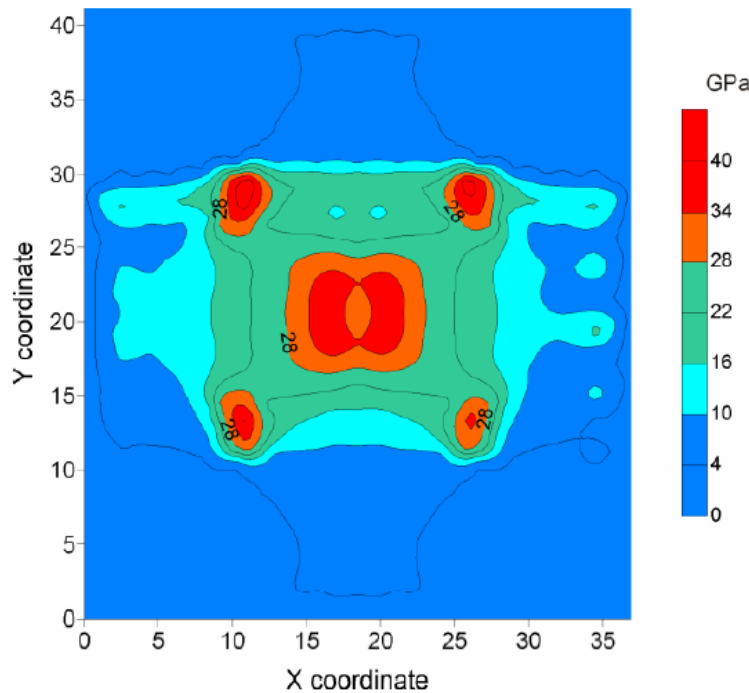
The deflection of the graphene sheet (620 atoms) by means of the platinum pyramid (376 atoms).



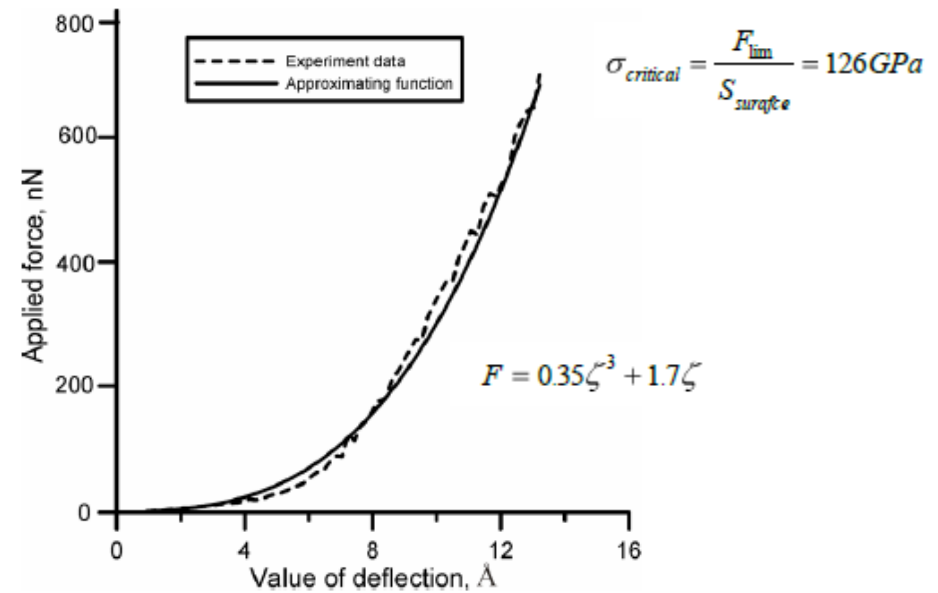
The image of the platinum pyramid and graphene sheet through 13.2 ps after the start of the experiment.



Picture of graphene sheet through 14.2 ps after the start of the experiment.

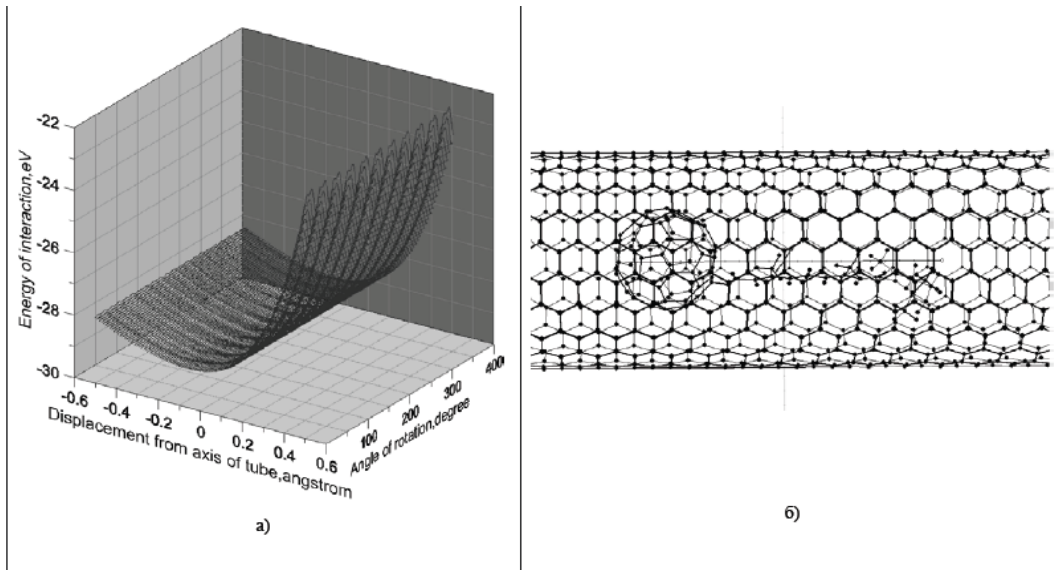


Map of the local stress, calculated through 13ps after the start of the experiment.



The dependence of the applied force on the bending deflection in the center of the upper plate bi-layer graphene plate. The dashed line corresponds to data obtained in the experiment, the solid - approximated function.

Fullerenes manipulations inside a carbon nanotube (hybrid compound Ret-C60 inside CNT)

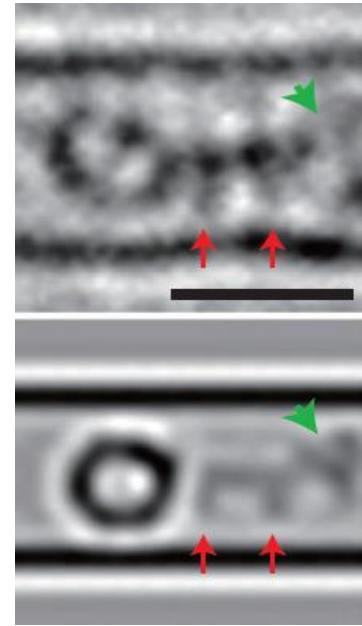


nanotube (11, 11).

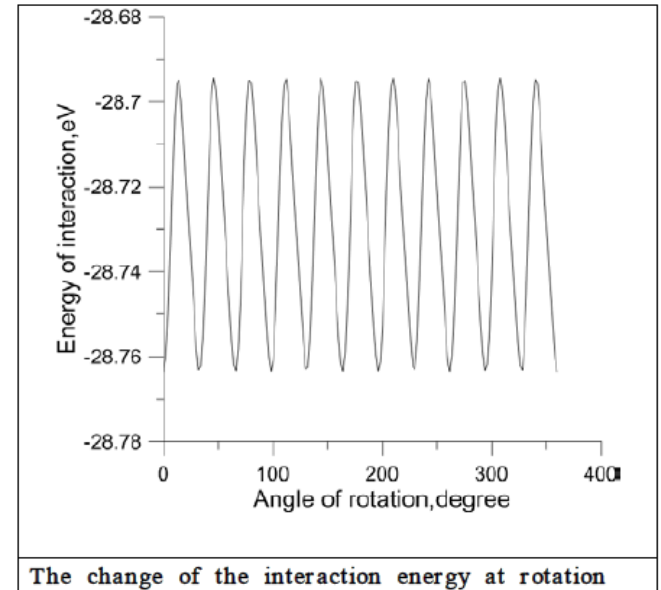
DFT method with exchange-correlation functional B3LYP

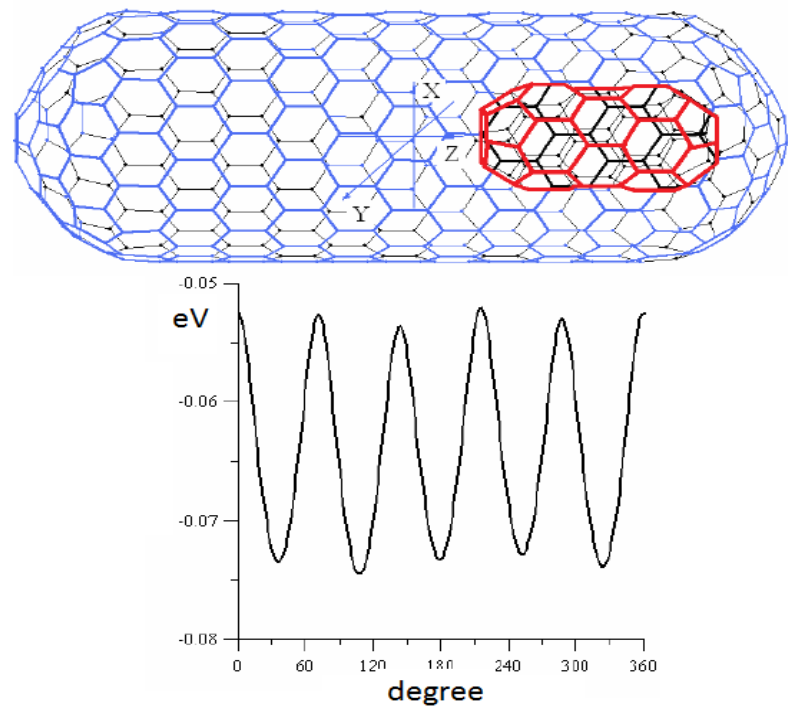
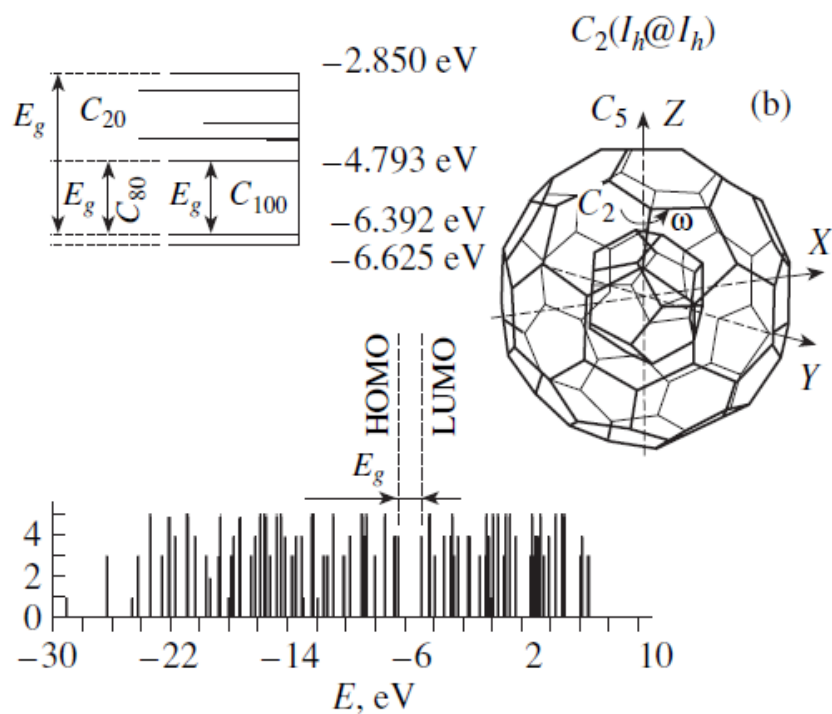
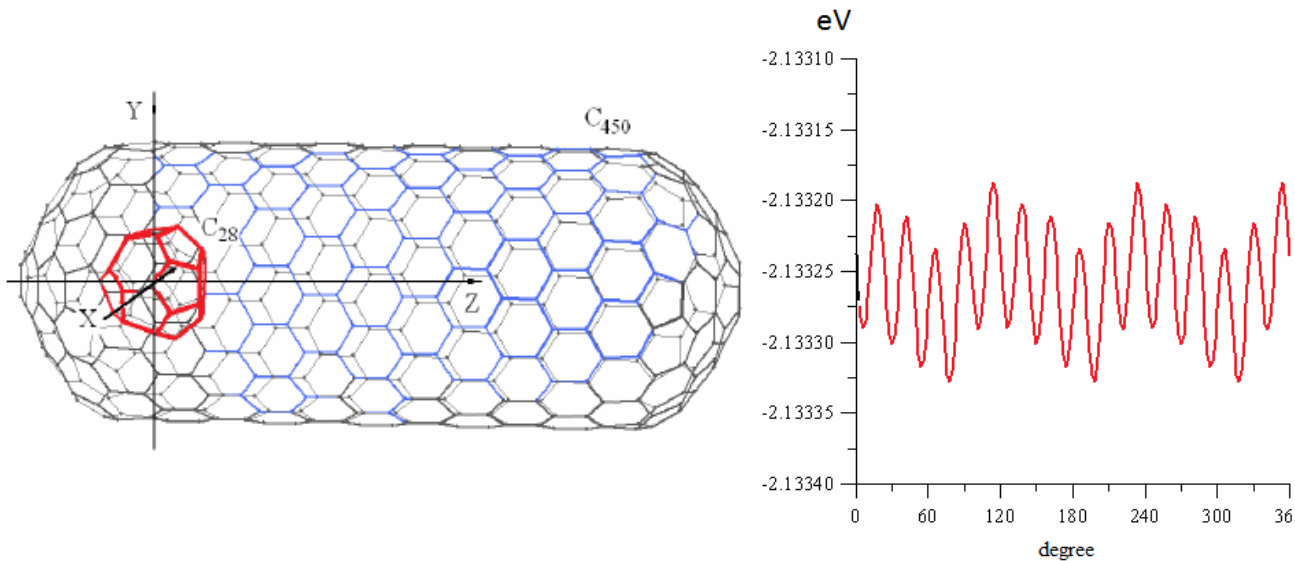
Retinol rotates with fullerene C60 freely when locating on the axis.

O.E. Glukhova, I.V. Kirillova, I.N. Saliy, M.M. Slepchenkov Single-fullerene manipulation inside a carbon nanotube // Proc. of SPIE Vol. 7911. doi: 10.1117/12.878677. – 2011.

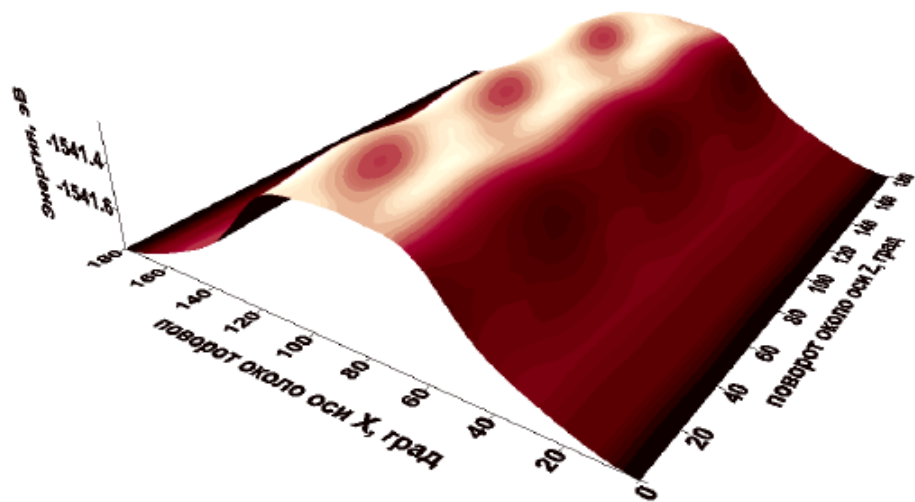
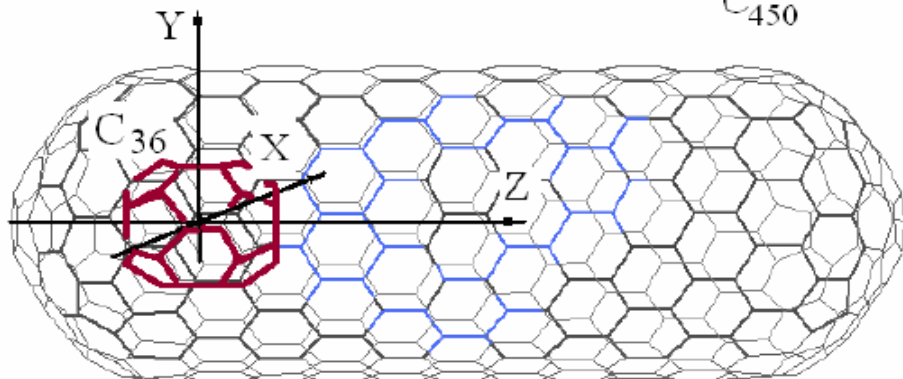


nature nanotechnology | VOL 2 | JULY 2007





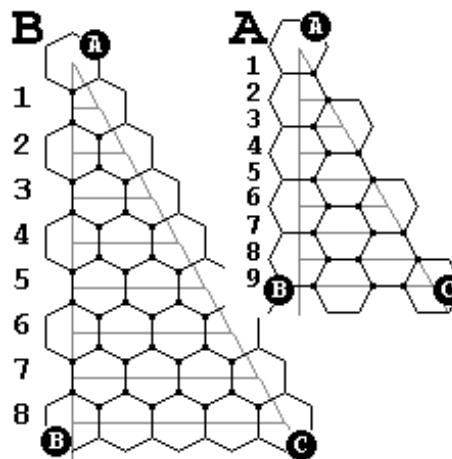
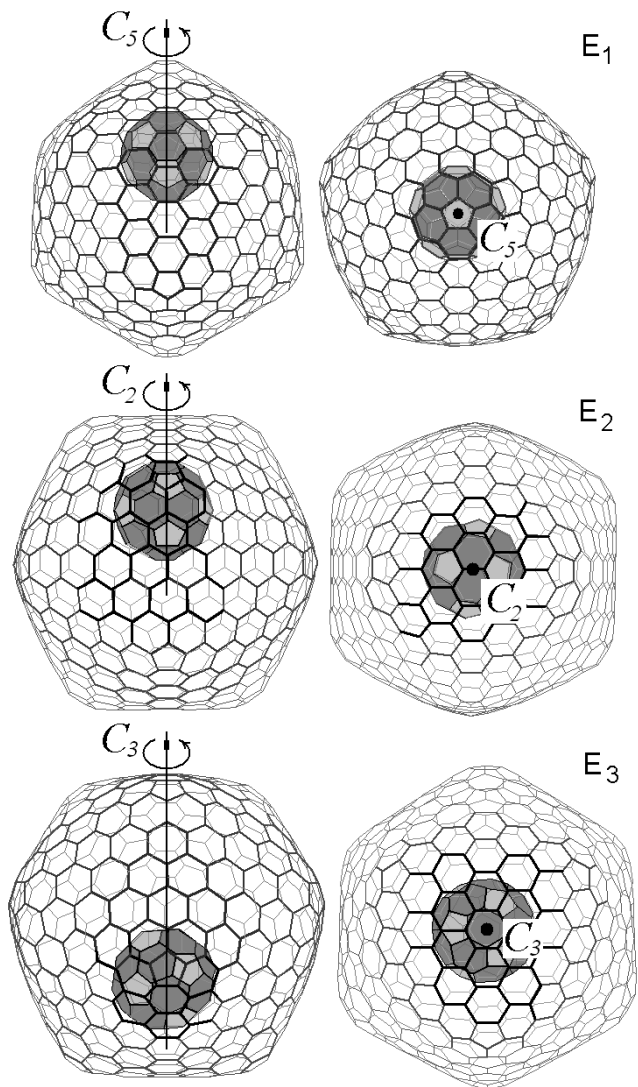
Glukhova, Zhanov, Rezkov // *Physics of the Solid State (Springer)*, Vol. 47, No. 2, 2005, pp. 390–396.
 O.E. Glukhova // *Journal of Structural Chemistry*. 2007. Vol. 48. SUPPL. 1. S. 141-146.

C_{450} 

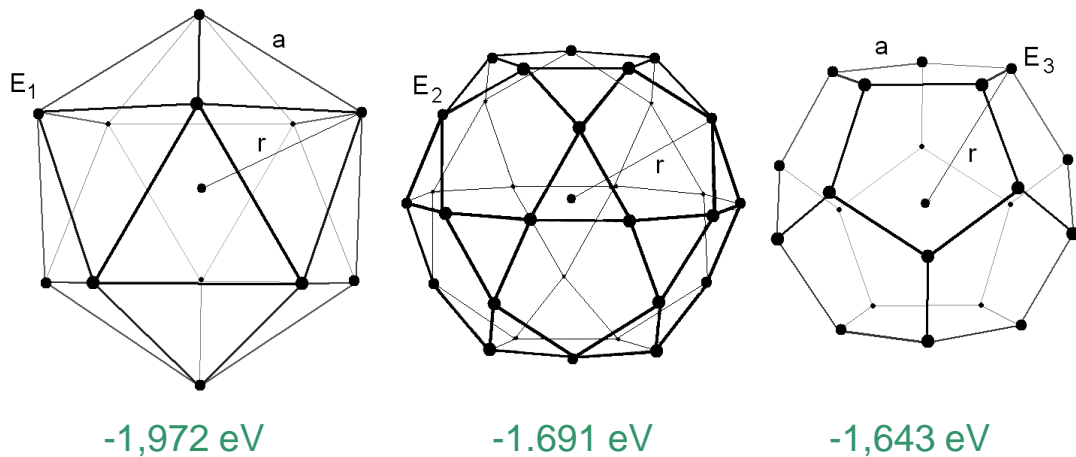
	$C_{28}(T_d)$ inside C_{168}	$C_{36}(D_{6d})$ inside C_{450}	$C_{28}(T_d)$ inside C_{450}	$C_{60}(D_{6d})$ inside C_{450}
k	cm^{-1}	cm^{-1}	cm^{-1}	cm^{-1}
0	77,8	46,3	19,9	34,9
+1	77,9	46,4	20,3	35,0
2	78,0	46,5	21,4	35,2
3	78,1	46,7	23,3	35,6
4	78,3	47,0	25,9	36,1
5	78,6	47,4	29,2	36,8
6	78,9	47,8	33,3	37,6
7	79,2	48,3	38,1	38,7
8	79,7	48,9	43,7	39,8
9	80,2	49,6	50,0	41,1
10	80,7	50,4	57,1	42,6
11	81,3	51,2	64,9	44,2
12	81,9	52,1	73,4	45,9

Icosahedral fullerenes

$C_{60}@C_{540}$

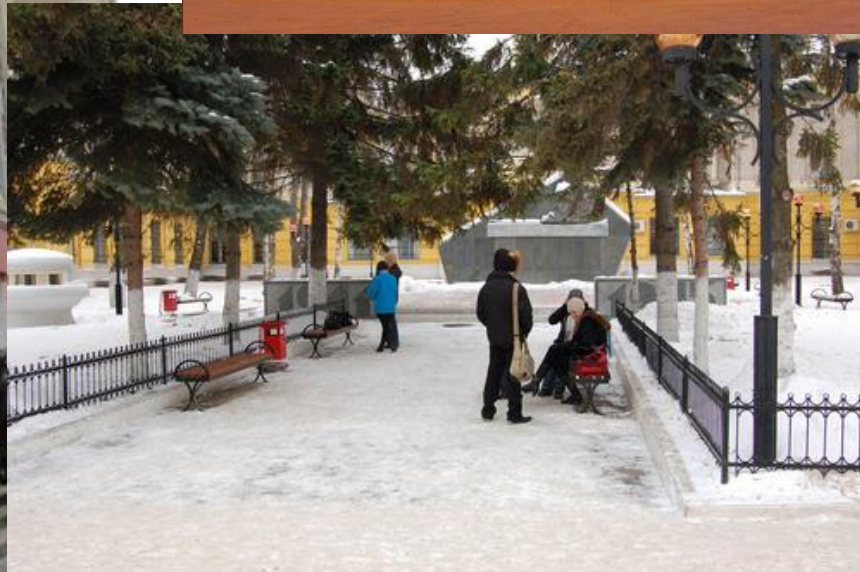
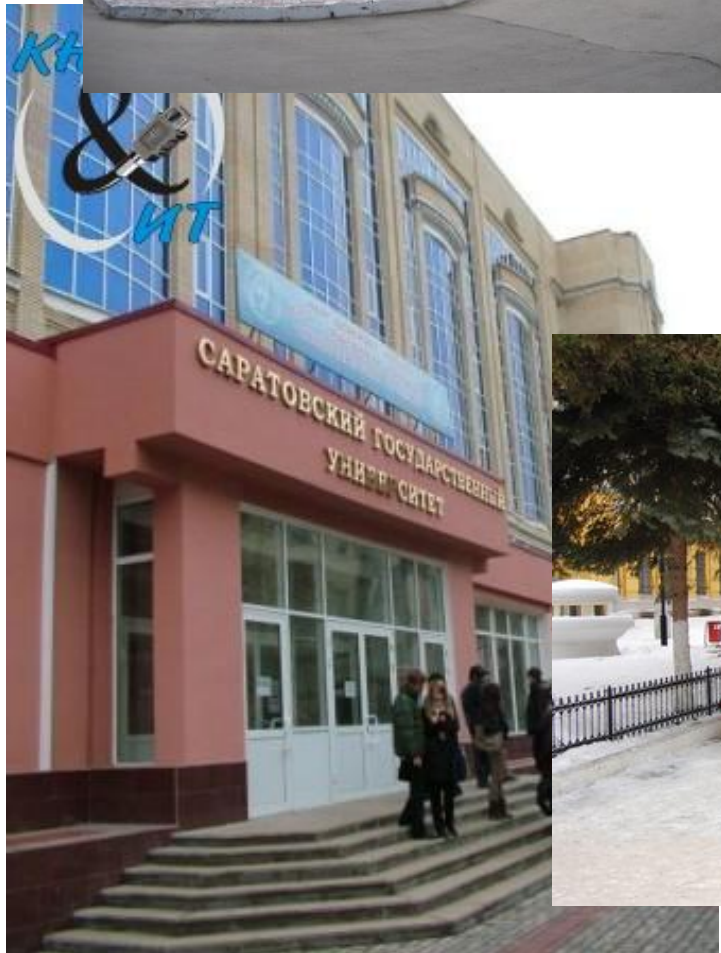


Topological models of fullerenes of icosahedral symmetry



Topology of multiwell potential

Saratov State University, www.sgu.ru







Thank you for your attention!